# The Disturbance Due to a Line Source in a Semi-Infinite Elastic Medium

E. R. Lapwood

| **Email alerting service** | Receive free email alerts when new articles cite this article - sign up in the box at the top right-hand corner of the article or click  **here** |
|---|---|

[ 63 ]

# THE DISTURBANCE DUE TO A LINE SOURCE IN A SEMI-INFINITE ELASTIC MEDIUM

By E. R. LAPWOOD, *Department of Geodesy and Geophysics, University of Cambridge, and Yenching University, Peiping West, China*

When a cylindrical pulse is emitted from a line source buried in a semi-infinite homogeneous elastic medium, the subsequent disturbance at any point near the surface is much more complex than for an incident plane pulse. The curvature of the wave-fronts produces diffraction effects, of which the Rayleigh-pulse is the most important.

In this paper the exact formal solution is given in terms of double integrals. These are evaluated approximately for the case when the depths of source and point of reception are small compared with their distance apart, allowing a description of the sequence of pulses which arrive at the point of reception. When that point is at the surface and distant from the epicentre, the disturbance there can be regarded as made up of the following pulses, in order of arrival: (*a*) for initial *P*-pulse at source: *P*-pulse, surface *S*-pulse and Rayleigh-pulse; (*b*) for initial *S*-pulse: surface *P*-pulse, *S*-pulse and Rayleigh-pulse. If the initial pulse has the form of a jerk in displacement, the *P*- and *S*-pulses arrive as similar jerks, whereas the Rayleigh-pulse is blunted, having no definite beginning or end. The surface *P*-pulse takes a minimum-time path and arrives with a jerk in velocity. The surface *S*-pulse, on the other hand, is confined to the neighbourhood of the surface and arrives as a blunted pulse. Moreover, part of the *S*-pulse arrives before the time at which it would be expected on geometrical theory.

Although derived on very restricting hypotheses, these results may throw some light on seismological problems. In particular, it is shown that when the sharp *S*-pulse of ray theory is converted by the presence of the surface *S*-pulse and the spreading of *S* into a blunted pulse, the duration of this composite pulse is of the same order of magnitude as the observed scatter of readings of *Sg* and other distortional pulses from near earthquakes.

## 1. INTRODUCTION

The propagation of tremors over the surface of a semi-infinite elastic solid* was first discussed by Lamb (1904) in a classic paper. He considered the surface displacements at a distant point which occur as a result of the application of a vertical or horizontal impulse along a line in the surface. He was able to demonstrate, after intricate analysis, that the required displacement will show a sequence of *P*-pulse,† *S*-pulse and Rayleigh-pulse.

Lamb also indicated a method of attack for the case when the initial disturbance was located at a certain depth below the free surface of the solid. His method of obtaining the formal solution (involving a double integration) is used in §§ 4 and 5 below, though the disturbance here considered differs in type from his. Lamb showed further that the solution for the corresponding three-dimensional problem follows in general that of the two-dimensional one.

* I am much indebted to Professor Harold Jeffreys, who proposed the subject of this paper and has given valuable advice.

† Throughout the following work the abbreviations '*P*-pulse' and '*S*-pulse' will be used to denote the longitudinal (irrotational) and transverse (distortional) pulses respectively.

Nakano (1925), confining his attention to the two-dimensional case, followed up Lamb's formulation of the solution when the line source lies below the surface, but carried out the approximate evaluation of the integrals by the methods of steepest descents and stationary phase. This gave more information about the displacements in the neighbourhood of the source, and a clearer analysis of the part played by each of the singularities of the integrands. Nakano concluded that there should be observed at a distant point on the free surface, due to an initial $P$-vibration, the direct $P$-wave, the Rayleigh-wave, and also a wave which had travelled along the surface with the velocity of an $S$-wave. When he replaced the initial harmonic vibration by a pulse of arbitrary form, and evaluated his integrals along a different path, he failed to find the 'surface $S$-wave'.

Similarly, examining the disturbances due to an original $S$-vibration, he obtained $S$-wave, Rayleigh-wave, and 'surface $P$-wave'. In this case, generalization did show a 'surface $P$-pulse', which, in contradistinction to the 'surface $S$-pulse', does satisfy a minimum-time criterion.
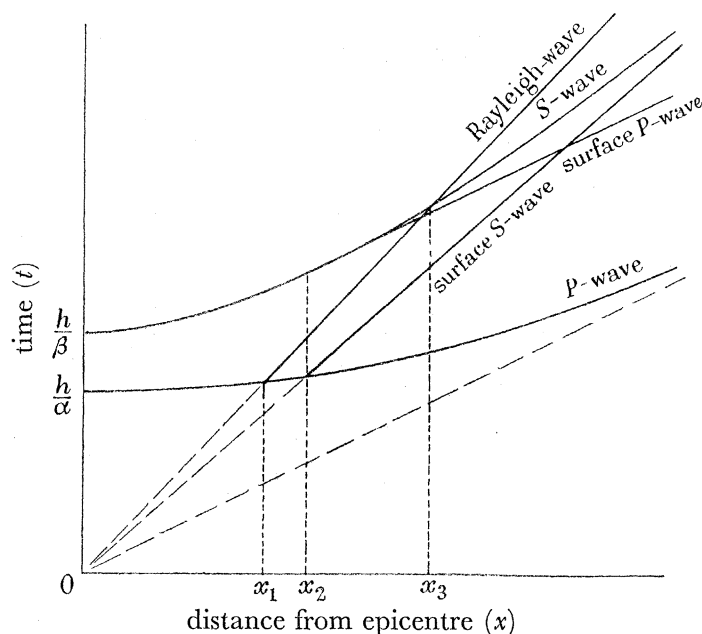


FIGURE 1. Time curves predicted by Nakano.

$$x_1 = \gamma h/\sqrt{(\alpha^2 - \gamma^2)}, \quad x_2 = \beta h/\sqrt{(\alpha^2 - \beta^2)}, \quad x_3 = \gamma h/\sqrt{(\beta^2 - \gamma^2)}$$

where $h$ is the depth of focus and $\alpha$, $\beta$, $\gamma$, are velocities of $P$-, $S$- and Rayleigh-waves respectively.

Nakano drew the time curves shown in figure 1 to illustrate the relationship of the different pulses, for the case when the original source emits a pulse with both $P$- and $S$-components (explanatory notes have been added and a correction made). He concluded, however (1925, p. 324): 'when the distance becomes larger than $\beta h/\sqrt{(\alpha^2 - \beta^2)}$, two other components appear, which correspond to the straight lines (marked *surface S-wave* and *surface P-wave*). These are waves which are propagated along the surface, but they are not free surface waves in the strict sense. The existence of the surface $P$-wave is possible, but its commencement will not be sharp in comparison with those of irrotational and distortional waves. The reality of the surface $S$-wave (due to original $P$) is not certain, though it is obtained for the case when the motion is periodic and stationary.'

Muskat (1933) has attacked a similar problem—the reflexion and refraction of pulses at the interface between two layers of different elastic properties. While he obtains pulses like the 'surface $P$-pulse' and 'surface $S$-pulse' of Nakano, he has not discussed the displacements of a free surface in a semi-infinite homogeneous solid. Fu (1947) has recently published a brief investigation of the problem in three dimensions, confining his attention to the response to a point-source oscillating harmonically; the application of his results to earthquake phenomena is therefore uncertain.

Two considerations make it desirable to undertake a further investigation of this problem. The first is the divergence of Nakano's results from those given by geometrical theory and their uncertainty (see Byerly 1940). The second is the difficulty of reading all $S$-phases in the records of near earthquakes. Jeffreys (1946) writes: 'The large scatter of the readings of $S$ in normal earthquakes up to $20°$ is still unexplained; it is clear that the large movements read as $S$ by most observers are not $S$, but we still do not know what they are.'

An investigation of the nature of the surface $S$-wave, if it exists, should help towards the clearing up of this question.

In the following discussion, the problem of the disturbance near the surface of a semi-infinite medium is set up and solved for the case when the line-source emits a pulse of the form of a Heaviside unit function. In order to facilitate examination of the ensuing displacement, irrotational and distortional displacement-potentials are kept distinct, and evaluated for an arbitrary point near the surface, but not necessarily on it.

The form of Riemann surface, and consequent distortion of contour, first introduced by Sommerfeld (1909) and applied to geophysical problems by Jeffreys (1926 $a$, 1931), proves to give more convenient analysis than that of Lamb or Nakano.

## 2. PRELIMINARY ANALYSIS

While any disturbance which is a function of the time can be regarded either as a combination of waves of different periods and amplitudes, or as a combination of unit functions of different instants and amplitudes, the latter view is much the more suitable for our purpose. For a simple harmonic oscillation of infinite duration is totally inadequate as a representation of an earthquake source, whereas Jeffreys has shown (1931) that a simple unit function and the response to it give results 'probably valid for a wide class of earthquakes'.

We therefore seek the response to an initial disturbance in the form of a unit function

$$H(t) = \frac{1}{2\pi i} \int_\Omega e^{i\omega t} \frac{d\omega}{\omega} = 0, \; t < 0, \atop = 1, \; t > 0, \qquad (2\cdot1)$$

where $\Omega$ is the line parallel to the real axis in the $\omega$-plane running from $-\infty - ic$ to $+\infty - ic$, or any equivalent contour.

If in any system the response to an initial disturbance $e^{i\omega t}$ is $f(\omega)$, then by the principle of superposition the response to $H(t)$ will be

$$\frac{1}{2\pi i} \int_\Omega f(\omega) \frac{d\omega}{\omega}, \qquad (2\cdot2)$$

provided $f(\omega)$ is analytic in the region containing the contour $\Omega$, and the integral converges. In some cases, $(2\cdot2)$ may be evaluated by the usual methods; in particular, from Hankel's

contour integral for the factorial (Gamma) function we obtain the results (Copson 1935, p. 226)

$$\frac{1}{2\pi i}\int_\Omega \omega^{-\frac{3}{2}} e^{i\omega\tau}\, d\omega = 2(i\tau)^{\frac{1}{2}} \pi^{-\frac{1}{2}} H(\tau), \quad \frac{1}{2\pi i}\int_\Omega \omega^{-\frac{5}{2}} e^{i\omega\tau}\, d\omega = \tfrac{4}{3}(i\tau)^{\frac{3}{2}} \pi^{-\frac{1}{2}} H(\tau). \tag{2.3}$$

We shall meet, however, responses to $e^{i\omega\tau}$ of which the following definition is typical:

$$f(\omega) = \omega^n e^{\pm p\omega + i\omega\tau} \quad (n, p, \tau \text{ real}, p>0) \text{ according as } \mathscr{R}(\omega) \lessgtr 0, \tag{2.4}$$

except within the very acute sector bounded by $\arg\omega = -\tfrac{1}{2}\pi \pm \epsilon$, $\epsilon$ being small. In that sector $f(\omega)$ is represented not by (2.4) but by a function which makes a rapid but continuous transition from $\omega^n e^{+p\omega+i\omega\tau}$ on the left to $\omega^n e^{-p\omega+i\omega\tau}$ on the right of the sector (see §§ 11, 12, 14). Unfortunately, the contribution to (2.2) from the part of $\Omega$ which traverses this small sector is important but difficult to evaluate. Since, however, $f(\omega)$ is analytic in the lower half of the $\omega$-plane and $f(\omega)/\omega \to 0$ as $\omega \to \pm \infty$, we may replace $\Omega$ by the more convenient contour $\Omega'$, which proceeds from $-\infty$ to the origin and thence to $+\infty$ by two loops below the real axis and avoiding the sector $\arg\omega = -\tfrac{1}{2}\pi \pm \epsilon$. On $\Omega'$ the integral converges provided $n>0$, and (2.4) is valid right up to the origin. Then by use of

$$\int_0^\infty \omega^{n-1} e^{-p\omega} \frac{\cos}{\sin}\, \omega\tau\, d\omega = \Gamma(n)\, (p^2+\tau^2)^{-\frac{1}{2}n} \frac{\cos}{\sin}\, n\psi, \tag{2.5}$$

where $\psi = \tan^{-1} \tau/p$ (Stewart 1940, p. 503), we obtain the value of (2.2) as

$$\frac{1}{2\pi i}\Gamma(n)\, (p^2+\tau^2)^{-\frac{1}{2}n} \left[e^{in\psi} - e^{-in(\psi+\pi)}\right]. \tag{2.6}$$

We shall use the following results, obtained by inserting particular values of $n$ in (2.6) and in the corresponding formula for $f(\omega) = \mp \omega^n e^{\pm p\omega + i\omega\tau}$:

| Response to $e^{i\omega t}$ | Response to $H(t)$ | |
|---|---|---|
| $i\omega\, e^{\pm p\omega + i\omega\tau}$ | $\dfrac{1}{\pi}\dfrac{p}{p^2+\tau^2}$ | (2.7) |
| $\mp \omega\, e^{\pm p\omega + i\omega\tau}$ | $\dfrac{1}{\pi}\dfrac{\tau}{p^2+\tau^2}$ | (2.8) |
| $i^{\frac{1}{2}}\omega^{\frac{1}{2}}\, e^{\pm p\omega + i\omega\tau}$ | $(\pi p)^{-\frac{1}{2}} \cos^{\frac{1}{2}} \psi \sin(\tfrac{1}{2}\psi + \tfrac{1}{4}\pi)$ | (2.9) |
| $\mp i^{-\frac{1}{2}}\omega^{\frac{1}{2}}\, e^{\pm p\omega + i\omega\tau}$ | $(\pi p)^{-\frac{1}{2}} \cos^{\frac{1}{2}} \psi \sin(\tfrac{1}{2}\psi - \tfrac{1}{4}\pi)$ | (2.10) |

$\psi$ being given by $\tan\psi = \tau/p$.

## 3. Equations of motion, boundary conditions and displacement potentials

Let $z=0$ be the bounding plane of a semi-infinite medium of isotropic elastic material of density $\rho$ and elastic constants $\lambda$ and $\mu$. Choose the axes so that the line source $F$ which lies parallel to and at a depth $h$ below $z=0$ is given by $x=0$, $z=h$. We wish to discuss the disturbance at a point $G$, distant from $F$ and near to the surface $z=0$, due to a cylindrical pulse emitted from the line-source $F$.

Let $(u, w)$ be the displacements of the point $(x, z)$ in the $(x, z)$ plane. Then the equations of motion, in the absence of body forces (Bromwich 1898 has shown that gravity can be neglected in this problem), are

$$(\lambda + \mu) \, \partial\Delta/\partial x + \mu \nabla^2 u = \rho \, \partial^2 u / \partial t^2, \quad (\lambda + \mu) \, \partial\Delta/\partial z + \mu \nabla^2 w = \rho \, \partial^2 w / \partial t^2, \tag{3.1}$$

where $\Delta = \partial u/\partial x + \partial w/\partial z$ (Love 1906).

At the free surface, $z = 0$, the normal and tangential components of stress must vanish, i.e. $Z_z = 0$, $Z_x = 0$, giving

$$\lambda(\partial u/\partial x + \partial w/\partial z) + 2\mu \, \partial w/\partial z = 0, \quad \partial u/\partial z + \partial w/\partial x = 0, \quad \text{when } z = 0. \tag{3.2}$$

In general, the displacement of any point may be expressed as the sum of the gradient of a scalar potential and the curl of a vector potential, the former corresponding to an irrotational strain, and the latter to shearing strains only. Thus, in the two-dimensional case, we may introduce displacement-potentials $\Phi$, $\Psi$, writing

$$u = \Phi_x + \Psi_z, \quad w = \Phi_z - \Psi_x, \tag{3.3}$$

where suffixes denote partial differentiation. Substituting these expressions into the equations of motion (3.1), and the boundary conditions (3.2) we obtain

$$\nabla^2 \Phi = \frac{1}{\alpha^2} \frac{\partial^2 \Phi}{\partial t^2}, \quad \nabla^2 \Psi = \frac{1}{\beta^2} \frac{\partial^2 \Psi}{\partial t^2}, \quad \text{where} \quad \nabla^2 \equiv \frac{\partial^2}{\partial x^2} + \frac{\partial^2}{\partial z^2} \tag{3.4}$$

and $\alpha^2 = (\lambda + 2\mu)/\rho$, $\beta^2 = \mu/\rho$, so that $\alpha$, $\beta$ are the velocities of propagation of $P$- and $S$-waves respectively, with

$$\begin{aligned} \lambda\Phi_{xx} + (\lambda + 2\mu) \, \Phi_{zz} - 2\mu\Psi_{xz} = 0 \quad \text{(vanishing of normal stress),} \\ 2\Phi_{xz} + \Psi_{zz} - \Psi_{xx} = 0 \quad \text{(vanishing of tangential stress),} \end{aligned} \right\} \tag{3.5}$$

when $z = 0$.

## 4. Formal solution for initial $P$-pulse

We next construct a function which shall represent a pulse travelling out cylindrically from the line-source. The appropriate solution of the wave equation for $\Phi$ (3.4) which varies with time as $e^{i\omega \tau}$ may be written

$$\phi_0 = \pi i H i_0(\varpi \kappa_\alpha) \, e^{i\omega t}, \tag{4.1}$$

where

$$\kappa_\alpha = \omega/\alpha \quad \text{and} \quad \varpi^2 = x^2 + (h - z)^2, \tag{4.2}$$

and $Hi_0$ is the Hankel function of the second kind of zero order (Jeffreys & Jeffreys 1946, p. 544). This function is chosen from the various Bessel functions of zero order because when $|\varpi \kappa_\alpha|$ is large

$$Hi_0(\varpi \kappa_\alpha) \sim \sqrt{\frac{2i}{\pi \varpi \kappa_\alpha}} \, e^{-i\varpi \kappa_\alpha}, \tag{4.3}$$

and so $Hi_0(\varpi \kappa_\alpha) \, e^{i\omega t}$ will represent a wave travelling outwards with velocity $\alpha$. The factor $\pi i$ is introduced for algebraic convenience. We note that $Hi_0(z) \to 0$ as $|z| \to \infty$ providing $\mathscr{I}(z) \leqslant 0$.

Superposing such solutions, we find that when the time variation of the source is to be not as $e^{i\omega \tau}$ but as $H(t)$, the corresponding displacement potential is

$$\Phi_0 = \frac{1}{2} \int_\Omega Hi_0(\varpi \kappa_\alpha) \, e^{i\omega t} \frac{d\omega}{\omega}. \tag{4.4}$$

Inserting in (4·4) the relationship

$$Hi_0(\varpi\kappa_\alpha) = \frac{2i}{\pi}\int_0^\infty e^{-i\varpi\kappa_\alpha\cosh u}\, du, \tag{4·5}$$

which is valid for $\mathscr{I}(\omega) < 0$ (Jahnke & Emde 1945, p. 150), we obtain

$$\Phi_0 = \frac{i}{\pi}\int_\Omega \frac{d\omega}{\omega}\int_0^\infty e^{i\omega(t-(\varpi/\alpha)\cosh u)}\, du$$

$$= -2\cosh^{-1}(\alpha t/\varpi)\, H(t-\varpi/\alpha). \tag{4·6}$$

We proceed to examine the form of the displacement given exactly by (4·6) in order to be able to check the accuracy of methods of approximation which are used later. Since $\Phi_0$ is the displacement-potential of a $P$-pulse, the displacement at a distance $\varpi$ from the source is in the direction of the radius vector $\varpi$ and is given by

$$U_\varpi = \frac{\partial\Phi_0}{\partial\varpi} = \frac{2\alpha t}{\varpi\sqrt{(\alpha^2 t^2 - \varpi^2)}}\, H\!\left(t - \frac{\varpi}{\alpha}\right). \tag{4·7}$$

This displacement falls from $\infty$ at $t = \varpi/\alpha$ and approaches the limit $2/\varpi$ as $t \to \infty$. Writing $t = \varpi/\alpha + \tau$ we get, for small values of $\alpha\tau/\varpi$,

$$U_\varpi = \sqrt{\frac{2}{\varpi\alpha\tau}}\left(1 + \frac{\alpha\tau}{\varpi}\right)\left(1 + \frac{\alpha\tau}{2\varpi}\right)^{-\frac{1}{2}} H(\tau).$$
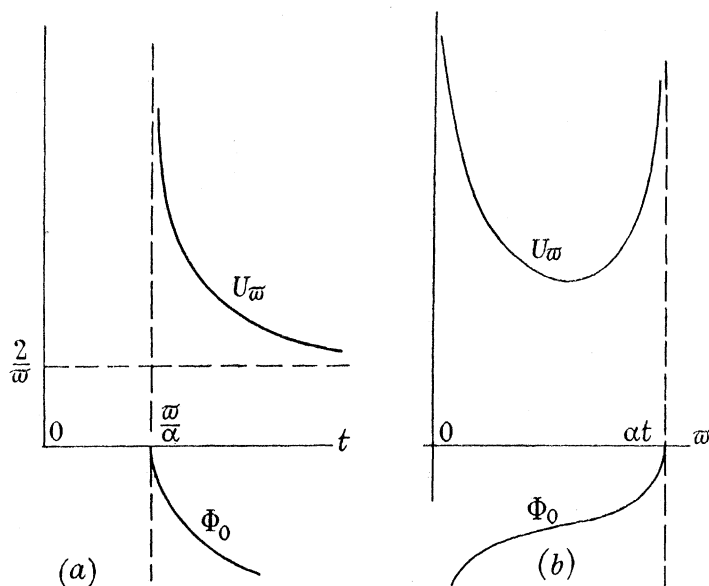


FIGURE 2. $\Phi_0$ and $U_\varpi$ graphed (a) against $t$, (b) against $\varpi$.

In figure 2, $\Phi_0$ and $U_\varpi$ are graphed (a) against $t$ for fixed $\varpi$, and (b) against $\varpi$ for given $t$. The displacement may be described as a sudden jerk at $t = \varpi/\alpha$, followed by a gradual recovery, which is incomplete. The residual displacement varies inversely as the distance. The infinity at $t = \varpi/\alpha$ represents a failure of the Hankel function to correspond to physical conditions, as does the infinity at $\varpi = 0$. The 'infinite tail' characterizes the solution of the wave equation in two dimensions (Jeffreys & Jeffreys 1946, p. 565; Lamb 1904, p. 28).

When the original disturbance is not a $P$- but an $S$-pulse, (4·4) is replaced by

$$\Psi_0 = \frac{1}{2}\int_\Omega Hi_0(\varpi\kappa_\beta)\, e^{i\omega t}\frac{d\omega}{\omega},\qquad(4\cdot8)$$

and (4·6) by

$$\Psi_0 = -2\cosh^{-1}(\beta t/\varpi)\, H(t-\varpi/\beta),\qquad(4\cdot9)$$

where $\kappa_\beta = \omega/\beta$. In this case the displacement at a distance $\varpi$ is

$$W_\varpi = -\frac{\partial\Psi_0}{\partial\varpi} = -\frac{2\beta t}{\varpi\sqrt{(\beta^2 t^2-\varpi^2)}}H\!\left(t-\frac{\varpi}{\beta}\right),$$

and is at right angles to the radius vector $\varpi$.

The expressions (4·4) and (4·8) for $\Phi_0$ and $\Psi_0$ respectively thus represent fairly well the disturbances in an infinite medium due to an initial explosion or twist at the line-source. Unfortunately, they are unsuitable for our problem, since the second derivatives which arise in the boundary conditions lead to very clumsy expressions. The difficulty lies in the occurrence of both $x$ and $z$ under the radical in $\varpi = \sqrt{[x^2+(h-z)^2]}$. We therefore seek a transformation of $Hi_0(\varpi\kappa_\alpha)$ into a form which contains $x$ and $z$ in linear combination, extending a result due to Lamb (1904, p. 4).

As in (4·5)
$$Hi_0(z\kappa_\alpha) = \frac{2i}{\pi}\int_0^\infty e^{-iz\kappa_\alpha\cosh u}\,du \quad\text{provided}\quad \mathscr{I}(z\kappa_\alpha)<0.\qquad(4\cdot10)$$

Write $i\kappa_\alpha\sinh u = \zeta$, $i\kappa_\alpha\cosh u = \lambda_\alpha$, so that $\lambda_\alpha du = d\zeta$ and $\lambda_\alpha^2 = \zeta^2-\kappa_\alpha^2$. Then

$$Hi_0(z\kappa_\alpha) = \frac{2i}{\pi}\int_0^{\infty i\kappa_\alpha} e^{-z\lambda_\alpha}\frac{d\zeta}{\lambda_\alpha},\qquad(4\cdot11)$$

and for real $z>0$, since $\cosh u$ is real and positive all along the original path of integration, we must choose the sign of $\lambda_\alpha$ so that $\mathscr{R}(\lambda_\alpha) = \cosh u\,\mathscr{R}(i\kappa_\alpha)>0$. This being so, we can replace the path of integration in (4·11) by the real axis from 0 to $\infty$, since the integral along the arc at infinity which connects the two paths is zero. This gives

$$Hi_0(z\kappa_\alpha) = \frac{2i}{\pi}\int_0^\infty e^{-z\lambda_\alpha}\frac{d\zeta}{\lambda_\alpha}\quad(z>0,\ \mathscr{I}(\omega)<0).\qquad(4\cdot12)$$

Now the solution of the wave equation for $\Phi$ (3·4) which is an even function of $x$ and reduces to $e^{-z\lambda_\alpha}e^{i\omega t}$ when $x=0$ is

$$e^{-z\lambda_\alpha}\cos\zeta x\, e^{i\omega t},$$

and so the solution which is an even function of $x$ and reduces to $\pi i Hi_0(z\kappa_\alpha)\,e^{i\omega t}$ when $x=0$ is

$$-2\int_0^\infty e^{-z\lambda_\alpha}\cos\zeta x\frac{d\zeta}{\lambda_\alpha}e^{i\omega t},$$

which must be identical with $\pi i Hi_0(\varpi_0\kappa_\alpha)\,e^{i\omega t}$ where $\varpi_0^2 = x^2+z^2$.

When the initial disturbance occurs not at the origin but at $x=0$, $z=h$, we can represent it by

$$\phi_0 = \pi i Hi_0(\varpi\kappa_\alpha)\,e^{i\omega t} = -2\int_0^\infty e^{-(h-z)\lambda_\alpha}\cos\zeta x\frac{d\zeta}{\lambda_\alpha}e^{i\omega t},\qquad(4\cdot13)$$

with $\varpi^2 = x^2 + (h-z)^2$ for the region $0 \leqslant z < h$ which concerns us. An equal source at the image point $(0, -h)$ will be given by

$$\phi_r = \pi i H i_0(\varpi' \kappa_\alpha) \, e^{i\omega t} = -2 \int_0^\infty e^{-(h+z)\lambda_\alpha} \cos \zeta x \frac{d\zeta}{\lambda_\alpha} e^{i\omega t}, \qquad (4 \cdot 14)$$

valid for $h > 0$, $z \geqslant 0$, where $\varpi'^2 = x^2 + (h+z)^2$.

We have proved $(4 \cdot 13)$ and $(4 \cdot 14)$ for $\mathscr{I}(\omega) < 0$, but they are also true in the limit when $\mathscr{I}(\omega) = 0$. In that case the branch-points $\lambda_\alpha = 0$ lie on the real axis, and the path of integration must be indented to pass above the branch-point on the positive half of the axis. Then the proof given by Lamb (1904, p. 4) becomes applicable.

Thus the complete expression for the initial $P$-pulse is

$$\Phi_0 = \frac{1}{2\pi i} \int_\Omega \frac{d\omega}{\omega} \int_0^\infty (-2) \, e^{-(h-z)\lambda_\alpha} \cos \zeta x \frac{d\zeta}{\lambda_\alpha} e^{i\omega t}. \qquad (4 \cdot 15)$$

We can now proceed to the formal solution of the problem. We shall work in terms of $\phi_0$ and obtain the solution for $\Phi_0$ by applying the operation $\dfrac{1}{2\pi i} \displaystyle\int_\Omega \dots \dfrac{d\omega}{\omega}$.

No set of image sources can balance both normal and tangential stress on $z = 0$, but we can nullify the normal stress by taking an equal and opposite source at $(0, -h)$. This gives a displacement potential

$$\phi_{0r} = \phi_0 - \phi_r = -4 \int_0^\infty e^{-h\lambda_\alpha} \sinh z\lambda_\alpha \cos \zeta x \frac{d\zeta}{\lambda_\alpha} e^{i\omega t}. \qquad (4 \cdot 16)$$

We now add further potentials $\phi$ and $\psi$ which are to be constructed so that all the conditions of the problem are satisfied by the potentials $\phi_{0r} + \phi$ and $\psi$.

Using the relation $(\lambda + 2\mu)/\mu = \kappa_\beta^2/\kappa_\alpha^2$ we can rewrite the boundary conditions $(3 \cdot 5)$ in the form

$$(\kappa_\beta^2 - 2\kappa_\alpha^2) \phi_{xx} + \kappa_\beta^2 \phi_{zz} - 2\kappa_\alpha^2 \psi_{xz} = 0, \quad 2\phi_{xz} + \psi_{zz} - \psi_{xx} = 0, \quad \text{when } z = 0. \qquad (4 \cdot 17)$$

At $z = 0$, $\qquad\qquad\qquad [\phi_{0r}]_{xx} = 0, \quad [\phi_{0r}]_{zz} = 0,$

$$[\phi_{0r}]_{xz} = 4 \int_0^\infty \zeta \, e^{-h\lambda_\alpha} \sin \zeta x \, d\zeta \, e^{i\omega t}. \qquad (4 \cdot 18)$$

The form of $(4 \cdot 18)$ suggests that $\phi$ and $\psi$ must be built up out of expressions like

$$\begin{matrix} \cos \\ \sin \end{matrix} \zeta x \, e^{\pm z\lambda_\alpha} \quad \text{and} \quad \begin{matrix} \cos \\ \sin \end{matrix} \zeta x \, e^{\pm z\lambda_\beta}, \quad \text{where} \quad \lambda_\beta^2 = \zeta^2 - \kappa_\beta^2. \qquad (4 \cdot 19)$$

The sign of $\lambda_\alpha$ is already determined, but that of $\lambda_\beta$ is at our disposal. Let us choose it so that $\mathscr{R}(\lambda_\beta) \geqslant 0$. Then in order to ensure that $\phi$ and $\psi$ vanish as $z \to \infty$ we must use the exponential multipliers $e^{-z\lambda_\alpha}$ and $e^{-z\lambda_\beta}$. This suggests for $\phi$ and $\psi$ the form

$$\phi = 4 \int_0^\infty (A \cos \zeta x + B \sin \zeta x) \, e^{-z\lambda_\alpha} \, d\zeta \, e^{i\omega t}, \qquad (4 \cdot 20)$$

$$\psi = 4 \int_0^\infty (C \cos \zeta x + D \sin \zeta x) \, e^{-z\lambda_\beta} \, d\zeta \, e^{i\omega t}. \qquad (4 \cdot 21)$$

Substituting from $(4 \cdot 20)$ and $(4 \cdot 21)$ into the boundary conditions we obtain two integrals which must be zero for every point of the boundary. We therefore equate the integrands

to zero, and since the coefficients of $\cos \zeta x$ and $\sin \zeta x$ must vanish separately, we obtain the equations for $A$, $B$, $C$, $D$:

$$(2\zeta^2 - \kappa_\beta^2)\, A + \qquad 2\zeta\lambda_\beta D = 0, \tag{4.22}$$

$$(2\zeta^2 - \kappa_\beta^2)\, B - \qquad 2\zeta\lambda_\beta C = 0, \tag{4.23}$$

$$2\zeta\lambda_\alpha A + (2\zeta^2 - \kappa_\beta^2)\, D = -2\zeta\, e^{-h\lambda_\alpha}, \tag{4.24}$$

$$-2\zeta\lambda_\alpha B + (2\zeta^2 - \kappa_\beta^2)\, C = 0, \tag{4.25}$$

(4.22) and (4.24) can be satisfied only if $F(\zeta) \neq 0$, where

$$F(\zeta) = (2\zeta^2 - \kappa_\beta^2)^2 - 4\zeta^2 \lambda_\alpha \lambda_\beta. \tag{4.26}$$

But if $F(\zeta) \neq 0$ we must have $B = 0$ and $C = 0$ to satisfy (4.23) and (4.25). Then solving for $A$ and $D$ and substituting we obtain

$$\phi = 16 \int_0^\infty \frac{\zeta^2 \lambda_\beta}{F(\zeta)}\, e^{-(h+z)\lambda_\alpha} \cos \zeta x \, d\zeta \, e^{i\omega t}, \tag{4.27}$$

$$\psi = -8 \int_0^\infty \frac{\zeta(2\zeta^2 - \kappa_\beta^2)}{F(\zeta)}\, e^{-h\lambda_\alpha - z\lambda_\beta} \sin \zeta x \, d\zeta \, e^{i\omega t}. \tag{4.28}$$

Hence the formal solution of the problem is given by the displacement potentials $\Phi_{0r} + \Phi$ and $\Psi$, where

$$_p\Phi_{0r} = \frac{1}{2\pi i} \int_\Omega e^{i\omega t} \frac{d\omega}{\omega} \int_0^\infty (-4)\, e^{-h\lambda_\alpha} \sinh \zeta \lambda_\alpha \cos \zeta x \frac{d\zeta}{\lambda_\alpha}, \tag{4.29}$$

$$_p\Phi = \frac{1}{2\pi i} \int_\Omega e^{i\omega t} \frac{d\omega}{\omega} \int_0^\infty \frac{16\zeta^2 \lambda_\beta}{F(\zeta)}\, e^{-(h+z)\lambda_\alpha} \cos \zeta x \, d\zeta, \tag{4.30}$$

and

$$_p\Psi = \frac{1}{2\pi i} \int_\Omega e^{i\omega t} \frac{d\omega}{\omega} \int_0^\infty \frac{(-8)\, \zeta\, (2\zeta^2 - \kappa_\beta^2)}{F(\zeta)}\, e^{-h\lambda_\alpha - z\lambda_\beta} \sin \zeta x \, d\zeta, \tag{4.31}$$

where the prefix $p$ means that these potentials refer to an original $P$-pulse.

## 5. FORMAL SOLUTION FOR INITIAL $S$-PULSE

When the original disturbance is an $S$-pulse, we start from the expression (4.8) for $\Psi_0$. By transformations identical with those of §4, except that $\beta$ replaces $\alpha$, we obtain

$$_s\Psi_{0r} = \frac{1}{2\pi i} \int_\Omega e^{i\omega t} \frac{d\omega}{\omega} \int_0^\infty (-4)\, e^{-h\lambda_\beta} \sinh z\lambda_\beta \cos \zeta x \frac{d\zeta}{\lambda_\beta}. \tag{5.1}$$

Substituting this into the boundary conditions, we find

$$_s\Phi = \frac{1}{2\pi i} \int_\Omega e^{i\omega t} \frac{d\omega}{\omega} \int_0^\infty \frac{8\zeta\, (2\zeta^2 - \kappa_\beta^2)}{F(\zeta)} \sin \zeta x \, e^{-h\lambda_\beta - z\lambda_\alpha} \, d\zeta, \tag{5.2}$$

$$_s\Psi = \frac{1}{2\pi i} \int_\Omega e^{i\omega t} \frac{d\omega}{\omega} \int_0^\infty \frac{16\zeta^2 \lambda_\alpha}{F(\zeta)} \cos \zeta x \, e^{-(h+z)\lambda_\beta} \, d\zeta. \tag{5.3}$$

We notice the strong resemblance between these expressions and (4.30) and (4.31), but the interchange of $\alpha$ and $\beta$ introduces remarkable differences in the interpretation of the integrals.

### 6. Poles of the integrands on the Riemann surface

Exact evaluation of the integrals along the $\zeta$-axis is impossible, and numerical calculation almost so. We therefore regard $\zeta$ as a complex variable, and distort the path of integration so as to concentrate the important contributions in certain sections. When the choice of signs in $\lambda_\alpha$ and $\lambda_\beta$ is unrestricted, the integrands are four-valued functions of $\zeta$, and their representation needs a four-leaved Riemann surface. The four leaves of this surface can be so defined as to correspond to the four possible sign-combinations of $\mathscr{R}(\lambda_\alpha)$ and $\mathscr{R}(\lambda_\beta)$. By our decision that $\mathscr{R}(\lambda_\alpha) > 0$, $\mathscr{R}(\lambda_\beta) > 0$, at all points of the path of integration, we have confined it to the leaf of the Riemann surface for which $\mathscr{R}(\lambda_\alpha) \geqslant 0$, $\mathscr{R}(\lambda_\beta) \geqslant 0$ everywhere. We shall call this the 'top leaf'.*

The branch-points are the four points $\zeta = \pm\kappa_\alpha, \pm\kappa_\beta$, at which $\lambda_\alpha = 0$ or $\lambda_\beta = 0$, and the cuts, along which the four leaves coalesce, must be given by $\mathscr{R}(\lambda_\alpha) = 0$, $\mathscr{R}(\lambda_\beta) = 0$. Let us write $\zeta = \xi + i\eta$, $\omega = s - ic$, then $\mathscr{R}(\lambda_\alpha) = 0$ implies that

$$\xi^2 - \eta^2 + 2i\xi\eta - (s^2 - c^2 - 2isc)/\alpha^2$$

is real and negative. Thus

$$\xi\eta = -sc/\alpha^2 \quad \text{and} \quad \xi^2 - \eta^2 < (s^2 - c^2)/\alpha^2,$$

and so the cuts from $\pm\kappa_\alpha$ must lie as shown in figure 3 along parts of a hyperbola which has the axes as asymptotes. Similarly, $\mathscr{R}(\lambda_\beta) = 0$ defines part of the hyperbola $\xi\eta = -sc/\beta^2$.
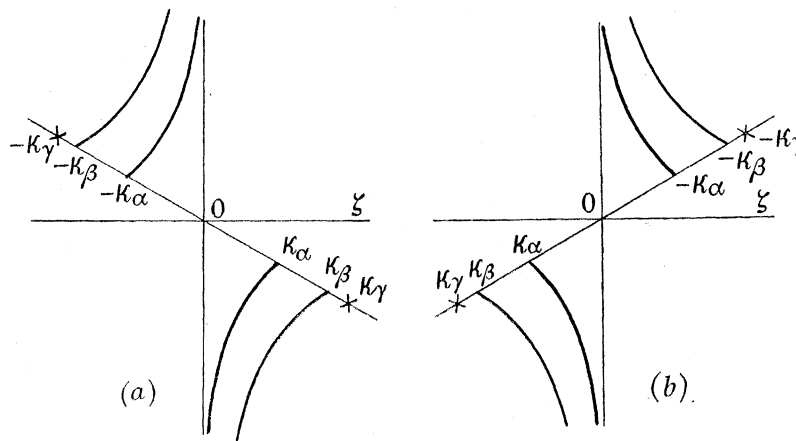


Figure 3. Branch-lines and poles in the $\zeta$-plane (a) $\mathscr{R}(\omega) > 0$ and (b) $\mathscr{R}(\omega) < 0$.

The integrands have poles at the zeroes of $F(\zeta)$. We now proceed to identify these poles, and to assign the appropriate ones to the top leaf of the Riemann surface.

The algebra is very greatly simplified if we now consider the special (Poisson) case in which the elastic constants $\lambda$ and $\mu$ are equal. This is nearly true for most rocks near the surface of the earth (Jeffreys 1929, p. 86). Small changes in $\lambda$ and $\mu$ would merely shift slightly in the $\zeta$-plane the positions of the zeroes of $F(\zeta)$; the conclusions reached below would still remain true.

---

\* This choice of Riemann surface follows naturally from our original expression for the Hankel function. A different convention of signs for the radicals will lead to a different Riemann surface, as in Lamb's paper (1904). Lamb, however (followed by Nakano), indented the path *above* the singular points on both sides of the origin, and as a result was forced to take principal values of the integrals and to add a free vibration in order to obtain progressive Rayleigh waves.

When $\lambda = \mu$, $\alpha^2 = 3\beta^2$, and $\kappa_\alpha = \kappa/\sqrt{3}$, where in this (Poisson) case we write $\kappa$ for $\kappa_\beta$. Then $F(\zeta) = 0$ gives

$$(2\zeta^2 - \kappa^2)^4 = 16\zeta^4(\zeta^2 - \kappa^2/3)(\zeta^2 - \kappa^2),$$

i.e.

$$\tfrac{32}{3}\kappa^2\left(\zeta^2 - \frac{\kappa^2}{4}\right)\left(\zeta^2 - \frac{3 - \sqrt{3}}{4}\kappa^2\right)\left(\zeta^2 - \frac{3 + \sqrt{3}}{4}\kappa^2\right) = 0. \tag{6.1}$$

Since (6.1) has been derived by squaring, not all its roots satisfy $F(\zeta) = 0$ on the top leaf of the Riemann surface. Considering them in turn we find that the only roots which lie on the top leaf are $\zeta = \pm(3 + \sqrt{3})^{\frac12}\kappa/2$. These will be denoted by $\pm\kappa_\gamma$. In the Poisson case $\kappa_\alpha = \kappa/\sqrt{3} = 0\cdot58\kappa$, and $\kappa_\gamma = (3 + \sqrt{3})^{\frac12}\kappa/2 = 1\cdot09\kappa$. The singularities on the top leaf of the Riemann surface are shown in figure 3, in the two cases (a) $\omega$ in the fourth quadrant, and (b) $\omega$ in the third quadrant.

## 7. DISTORTION OF PATH OF INTEGRATION

Henceforward we shall consider only the region $x > 0$. The analysis for the region $x < 0$ does not differ in any essential point, other than that all pulses travel in the opposite direction from the source.

Each of our integrals in the $\zeta$-plane is of one of the two forms

$$\chi_1 = \int_0^\infty G(\zeta)\cos\zeta x\, d\zeta, \tag{7.1}$$

$$\chi_2 = \int_0^\infty \zeta G(\zeta)\sin\zeta x\, d\zeta, \tag{7.2}$$

where $G(\zeta)$ is an even function of $\zeta$ containing a factor of such form as $e^{-h\lambda_\alpha - z\lambda_\beta}$ which vanishes exponentially on any arc of the circle at infinity, except possibly in the neighbourhood of the negative imaginary axis, where $G(\zeta)$ is $O(1/|\zeta|)$. Let us write

$$\chi_1 = \frac{1}{2}\int_0^\infty G(\zeta)\,e^{i\zeta x}\, d\zeta + \frac{1}{2}\int_0^\infty G(\zeta)\,e^{-i\zeta x}\, d\zeta, \tag{7.3}$$

$$\chi_2 = \frac{1}{2i}\int_0^\infty \zeta G(\zeta)\,e^{i\zeta x}\, d\zeta - \frac{1}{2i}\int_0^\infty \zeta G(\zeta)\,e^{-i\zeta x}\, d\zeta. \tag{7.4}$$

When $\zeta$ lies in the fourth quadrant, $e^{-i\zeta x} \to 0$ as $|\zeta| \to \infty$ provided $\mathscr{I}(\zeta) \neq 0$, and when $\zeta$ lies in the first quadrant, $e^{i\zeta x} \to 0$ as $|\zeta| \to \infty$, provided $\mathscr{I}(\zeta) \neq 0$. We now distort the contour, obtaining different results according as $\mathscr{R}(\omega) \gtrless 0$.

(i) $\mathscr{R}(\omega) > 0$

Distort the path in the first integrals of (7.3) and (7.4) into the positive imaginary axis together with the first quadrant of the infinite circle. Distort the path in the second integrals of (7.3) and (7.4) into the negative imaginary axis, together with a loop $\Gamma$ around the singularities and the fourth quadrant of the infinite circle (see figure 4 (a)). The contributions from the infinite arcs are zero, and we have

$$\chi_1 = \frac{1}{2}\int_0^{i\infty} G(\zeta)\,e^{i\zeta x}\, d\zeta + \frac{1}{2}\int_0^{-i\infty} G(\zeta)\,e^{-i\zeta x}\, d\zeta + \frac{1}{2}\int_\Gamma G(\zeta)\,e^{-i\zeta x}\, d\zeta, \tag{7.5}$$

$$\chi_2 = \frac{1}{2i}\int_0^{i\infty} \zeta G(\zeta)\,e^{i\zeta x}\, d\zeta - \frac{1}{2i}\int_0^{-i\infty} \zeta G(\zeta)\,e^{-i\zeta x}\, d\zeta - \frac{1}{2i}\int_\Gamma \zeta G(\zeta)\,e^{-i\zeta x}\, d\zeta. \tag{7.6}$$

By a change of variable we see that the integrals along the imaginary axis cancel, leaving

$$\chi_1 = \frac{1}{2}\int_{\Gamma} G(\zeta)\, e^{-i\zeta x}\, d\zeta, \tag{7.7}$$

$$\chi_2 = -\frac{1}{2i}\int_{\Gamma} \zeta G(\zeta)\, e^{-i\zeta x}\, d\zeta. \tag{7.8}$$
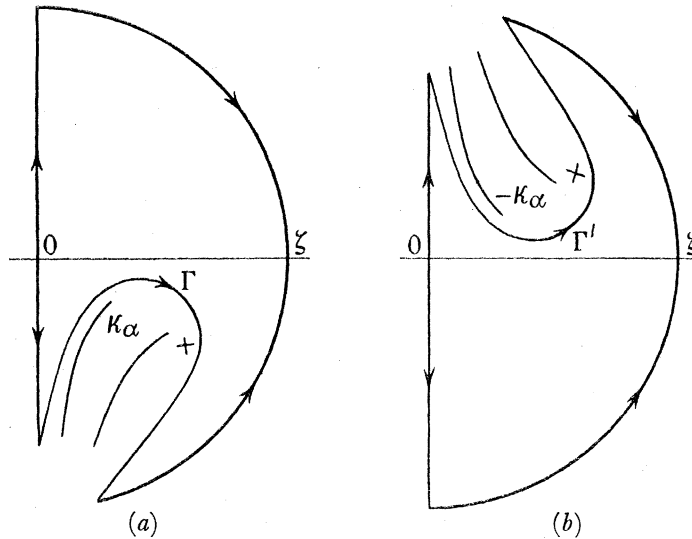


FIGURE 4. Distortion of contour in the $\zeta$-plane.   (a) $\mathscr{R}(\omega) > 0$.   (b) $\mathscr{R}(\omega) < 0$.

(ii)  $\mathscr{R}(\omega) < 0$

In this case the singularities on the right of the imaginary axis lie in the first quadrant, and the distorted path must include the loop $\Gamma'$ (see figure 4$b$) which contains the points $-\kappa_{\alpha}, -\kappa_{\beta}, -\kappa_{\gamma}$. (7.7) and (7.8) are replaced by

$$\chi_1 = \frac{1}{2}\int_{\Gamma'} G(\zeta)\, e^{i\zeta x}\, d\zeta, \tag{7.9}$$

$$\chi_2 = \frac{1}{2i}\int_{\Gamma'} \zeta G(\zeta)\, e^{i\zeta x}\, d\zeta. \tag{7.10}$$

Using the formulae (7.7) to (7.10) we obtain, for the case $\mathscr{R}(\omega) > 0$, the following expressions:

$$\phi_0 = -\int_{\Gamma} e^{-i\zeta x - (h-z)\lambda_{\alpha}} \frac{d\zeta}{\lambda_{\alpha}} e^{i\omega t}, \tag{7.11}$$

$$_p\phi = \int_{\Gamma} \frac{8\zeta^2 \lambda_{\beta}}{F(\zeta)} e^{-i\zeta x - (h+z)\lambda_{\alpha}}\, d\zeta\, e^{i\omega t}, \tag{7.12}$$

$$_p\psi = -\int_{\Gamma} \frac{4i\zeta(2\zeta^2 - \kappa_{\beta}^2)}{F(\zeta)} e^{-i\zeta x - h\lambda_{\alpha} - z\lambda_{\beta}}\, d\zeta\, e^{i\omega t}, \tag{7.13}$$

$$\psi_0 = -\int_{\Gamma} e^{-i\zeta x - (h-z)\lambda_{\beta}} \frac{d\zeta}{\lambda_{\beta}} e^{i\omega t}, \tag{7.14}$$

$$_s\phi = \int_{\Gamma} \frac{4i\zeta(2\zeta^2 - \kappa_{\beta}^2)}{F(\zeta)} e^{-i\zeta x - h\lambda_{\beta} - z\lambda_{\alpha}}\, d\zeta\, e^{i\omega t}, \tag{7.15}$$

$$_s\psi = \int_{\Gamma} \frac{8\zeta^2 \lambda_{\alpha}}{F(\zeta)} e^{-i\zeta x - (h+z)\lambda_{\beta}}\, d\zeta\, e^{i\omega t}, \tag{7.16}$$

and when $\mathscr{R}(\omega) < 0$, we get the same expressions, except that $i$ is replaced by $-i$, and the contour $\Gamma$ by $\Gamma'$.

When $\omega$ is real and positive, the contour takes the limiting form shown in figure 15. This may be proved by starting from the integral for $\phi_0$ when $\omega$ is real and following through the above argument with suitable modifications.

Again, when $\mathscr{R}(\omega) = 0$, $\Gamma$ becomes a simple loop from $-i\infty$ to $-i\infty$ enclosing the points $\kappa_\alpha$, $\kappa_\beta$ and $\kappa_\gamma$ on the negative axis of imaginaries, while $\Gamma'$ becomes the mirror image of $\Gamma$ in the real axis. The integrals along $\Gamma$ and $\Gamma'$ are then of course equivalent.

## 8. INTERPRETATION OF THE INTEGRALS

We now give a general picture of the meaning of the integrals (7·11) to (7·16), taking $\omega$ as fixed, $|\omega|$ not too small, $\arg \omega$ not too near 0 or $-\tfrac{1}{2}\pi$, and $x$ large compared with $h$ and $z$. This interpretation will indicate the approximate times taken by various waves to reach the point of reception, and something of their nature. It must, however, be treated with caution, as suggestive rather than definite, since it refers only to a single complex value of $\omega$, and it is not clear that the same interpretation will hold either in the limit when $\omega$ becomes real or pure imaginary, or when the exponential time variation is generalized into a pulse.

First we modify the contour $\Gamma$ further, transforming it as shown in figure 5 into three parts: $\Gamma_\alpha$, a loop lying indefinitely near to the branch-line $\mathscr{R}(\lambda_\alpha) = 0$; $\Gamma_\beta$, a similar loop around $\mathscr{R}(\lambda_\beta) = 0$; and $\Gamma_\gamma$, a small circle around the pole $\kappa_\gamma$.
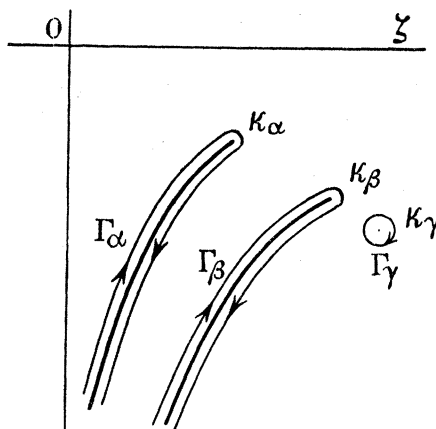


FIGURE 5. Further transformation of $\Gamma$.

We shall require $|\omega|$ to be large enough for the exponential factor to vary faster than its multiplier in each integrand, and $x/(z+h)$ to be large enough for us to take the variation of $e^{-ix\zeta}$ as dominating that of such factors as $e^{-h\lambda_\alpha - z\lambda_\beta}$ in the neighbourhood of the pole and branch-points.

If the point $\zeta$ describes the contour $\Gamma_\alpha$, the modulus of $e^{-ix\zeta}$ will take its largest value at $\kappa_\alpha$, and will decrease rapidly as $\zeta$ recedes from $\kappa_\alpha$ on either side of the branch-line. So the major contribution to the integral will come from the neighbourhood of $\kappa_\alpha$, and to a first approximation we shall have a factor $e^{i\omega(t-x/\alpha)}$. Thus we can say that the parts of the integrals which arise from this contour will represent waves which have travelled most of the way from the source to the point of reception with velocity $\alpha$. The type of displacement potential gives further information, and we may form the following conclusions (suffixes $\alpha$, $\beta$ and $\gamma$ denoting contributions from the loops $\Gamma_\alpha$, $\Gamma_\beta$ and $\Gamma_\gamma$ respectively).

(a) $_p\phi_\alpha$ represents a wave which started and finished as a $P$-wave and travelled most of the way with velocity $\alpha$. This must be a part of the reflected $P$-wave, $PP$.

(b) $_p\psi_\alpha$ is a wave which started as $P$ and finished as $S$ and travelled most of the way with velocity $\alpha$. Since we know from the reflexion of plane waves that the reflected $S$ from incident $P$ lies nearer the normal than the reflected $P$, this must be the reflected $S$-wave, $PS$.

(c) $_s\psi_\alpha$ is a wave which started and finished as an $S$-wave, but travelled most of the way with velocity $\alpha$, i.e. as a $P$-wave. Since the only place where transformations can take place is the surface, this must be the 'surface $P$-wave', $sPs$.

(d) $_s\phi_\alpha$ started as $S$ and finished as $P$, travelling most of the way with velocity $\alpha$. Since the reflected $P$-wave from incident $S$ is farther from the normal than the incident $S$, this must be the reflected $P$-wave, $SP$.



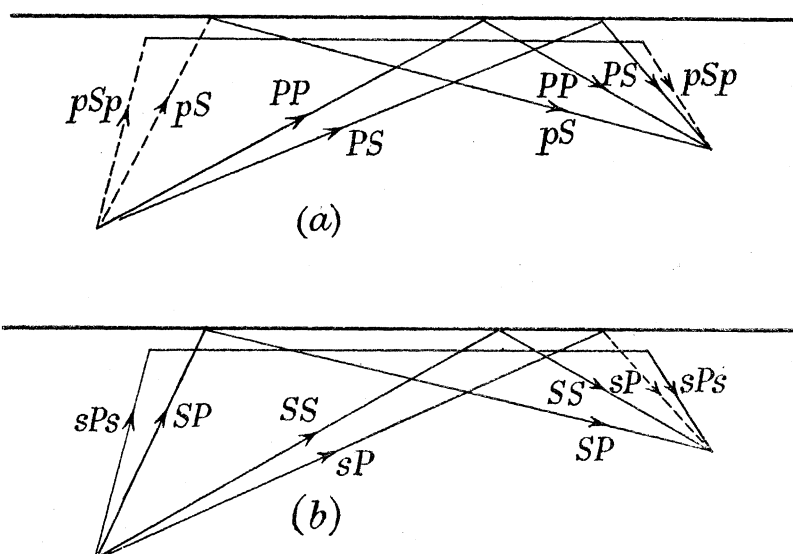FIGURE 6. Waves represented by integrals along $\Gamma_\alpha$ and $\Gamma_\beta$, (a) initial $P$-wave, (b) initial $S$-wave.

These four waves all correspond to minimum-time paths, i.e. their existence is also deducible by geometrical methods.

In the same way, we can analyze the contributions from the loop $\Gamma_\beta$, and see that these waves, which all travelled most of the way with velocity $\beta$, may be described as follows:

(e) $_p\phi_\beta$: this wave started and finished as $P$, but travelled most of the way as $S$. We may call it the 'surface $S$-wave' $pSp$, noting that, like the Rayleigh-wave, it satisfies no minimum-time criterion.

(f) $_p\psi_\beta$: this started as $P$ and finished as $S$, travelling most of the way with velocity $\beta$. It cannot be part of the wave $PS$, since it seems to have been reflected close to the epicentre. It will be called the 'secondary $S$-wave' $pS$. The path is not a minimum-time path.

(g) $_s\phi_\beta$: this corresponds to $(f)$, having started as $S$ and finished as $P$, travelling most of the way with velocity $\beta$. It is the 'secondary $P$-wave' $sP$, and has not a minimum-time path.

(h) $_s\psi_\beta$: this is part of the reflected $S$-wave, $SS$.

(i) The values of the contributions from $\Gamma_\gamma$ depend only on the residues at $\kappa_\gamma$, and so contain a factor $e^{i\omega(t-x/\gamma)}$. These waves therefore travel with velocity $\gamma$ and must be identified as the Rayleigh-waves, $R$. Longitudinal and transverse displacements arise in both cases.

Figure 6 gives a diagrammatic representation of the waves other than the Rayleigh-waves for (a) initial P-wave, and (b) initial S-wave. Of these waves, PP, PS, SS, SP arise in the case of reflexion of plane waves. The others are all diffraction effects due to the curvature of the wave-fronts which impinge on the free surface.

In this rough specification, we have been unable to make any statement concerning the amplitudes of the various waves, or even to assert that pulses corresponding to them will exist when the initial disturbance is a pulse. We now proceed to more detailed analysis, with the object of ascertaining the form of response to the initial unit pulse.

## 9. Paths of steepest descent and stationary phase

While the contour composed of $\Gamma_\alpha$, $\Gamma_\beta$ and $\Gamma_\gamma$ seems to lead to a convenient physical interpretation, it must not be assumed without further discussion that it will provide the best approximations to the values of the integrals. We shall now consider other possible contours, and for definiteness examine the behaviour of $_p\phi$ when $\mathscr{R}(\omega) > 0$. We shall not restrict ourselves to the case where $\theta$, defined by $(h+z)/x = \tan\theta$, is small. From (4.30), by a simple change of variable,

$$_p\phi = 8\int_{-\infty}^{\infty} \frac{\zeta^2 \lambda_\beta}{F(\zeta)}\, e^{-i\zeta x - (h+z)\lambda_\alpha + i\omega t}\, d\zeta. \tag{9.1}$$

Following the usual method of steepest descents, we can show that for the integral in (9.1) the path of steepest descent has the form shown by the continuous line in figure 7, where $H$ ($\zeta = \kappa_\alpha \cos\theta$) is the saddle-point.
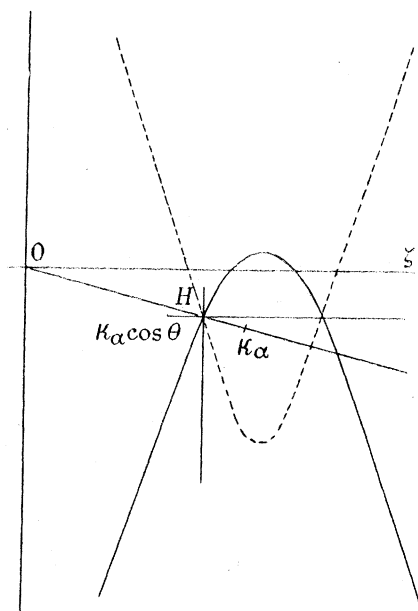


FIGURE 7. Path of steepest descent (continuous line).

When we attempt to distort the real axis into this path, the result depends on the value of $x/(h+z)$. Figure 8 shows how, as $x/(h+z)$ increases, the path of steepest descent resembles a parabola of decreasing latus rectum, closing in on the branch-point $\kappa_\alpha$. The distorted path of integration must not cross singularities, and so takes the form of figure 8 (a), (b) or (c)

according to the value of $x/(h+z)$. This analysis indicates that there are certain minimum distances at which the Rayleigh-wave and 'surface $S$-wave' first appear. Such a deduction was first made by Nakano (1925), but one of the puzzling statements in his work is that when he replaced the path of steepest descent by one of stationary phase no 'surface $S$-wave' appeared.
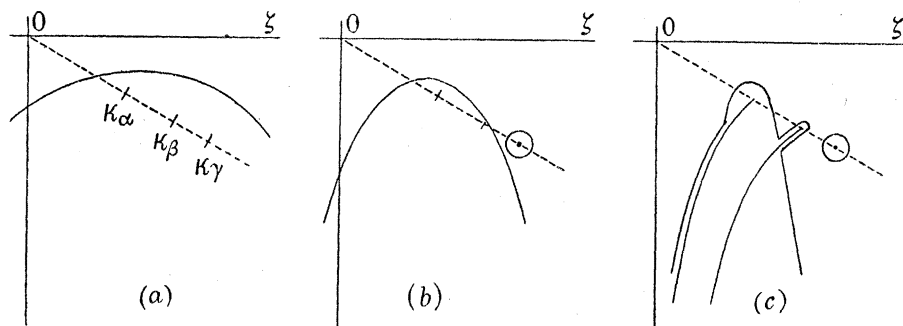


FIGURE 8. Modified line of steepest descent for $_p\phi$. (a) $x/(h+z) < \gamma/\sqrt{(\alpha^2 - \gamma^2)}$, (b) $\gamma/\sqrt{(\alpha^2 - \gamma^2)} < x/(h+z) < \beta/\sqrt{(\alpha^2 - \beta^2)}$, (c) $x/(h+z) > \beta/\sqrt{(\alpha^2 - \beta^2)}$.

An investigation has therefore been made into the form of the modified contour when distorted towards the path of stationary phase; the work parallels that described in the preceding paragraph, and the conclusion is that the same features emerge, including loops around $\kappa_\beta$ and $\kappa_\gamma$ under the same conditions on $x/(h+z)$.

When $x/(h+z)$ is large, the modifications to the path of steepest descent needed to avoid pole and branch-lines are so extensive that the path of steepest descent comes to resemble the Sommerfeld contour closely, except in the immediate neighbourhood of the saddle-point. The modified path of stationary phase, though it cannot be confined to the top leaf of the Riemann surface, also contains loops around $\kappa_\beta$ and $\kappa_\gamma$. The evaluations of the integral by the three methods should therefore show results agreeing in their main features, though they may differ in the accuracy of approximations obtainable.

## 10. EVALUATION OF INTEGRALS FOR REAL $\omega$

The loops $\Gamma_\alpha$ and $\Gamma_\beta$ are convenient for approximate evaluation of the integrals because we can find a new independent variable which takes only real values upon them. But since the saddle-points do not lie on these loops the results will lack the sharpness and accuracy of approximation obtained by steepest descent or stationary phase. If, however, we consider the limiting case when $\omega$ is real and positive, the contour of integration takes the form shown in figure 15 and the saddle-points lie upon it. We can therefore get useful information from this limiting case. First we give a more adequate justification of its employment than was given in passing in §§ 4 and 7.

We shall prove the formula

$$\int_{\Gamma_0} e^{-ix\zeta - (h-z)\lambda_\alpha} \frac{d\zeta}{\lambda_\alpha} = -\pi i H i_0(\varpi \kappa_\alpha), \tag{10.1}$$

where $\kappa_\alpha$ is real and positive; the other symbols have their usual meaning, and $\Gamma_0$ is the contour shown in figure 9. Writing $\lambda_\alpha = (\zeta - \kappa_\alpha)^{\frac{1}{2}} (\zeta + \kappa_\alpha)^{\frac{1}{2}}$, we see that $\mathscr{I}(\lambda_\alpha)$ vanishes on the real axis in $(-\infty, -\kappa_\alpha)$ and $(\kappa_\alpha, +\infty)$ and so changes sign in crossing these segments.

Near $\kappa_\alpha$, $\lambda_\alpha \doteqdot \sqrt{\{2\kappa_\alpha(\zeta - \kappa_\alpha)\}}$, and since $\mathscr{R}(\lambda_\alpha) \geqslant 0$ we prove easily that $\mathscr{I}(\lambda_\alpha)$ is positive above the real axis there, and negative below. It follows that $\mathscr{I}(\lambda_\alpha)$ takes on $\Gamma_0$ the signs shown in figure 9.
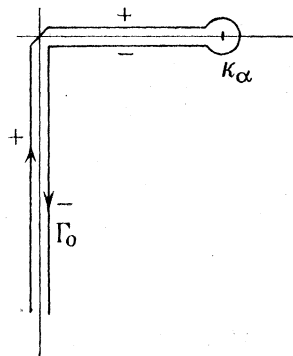


FIGURE 9. The contour $\Gamma_0$.

Then in the left-hand member of equation (10·1) let us write $x = \varpi \cos\theta$, $h - z = \varpi \sin\theta$, $\zeta = \kappa_\alpha \cos\vartheta$, $\lambda_\alpha = \pm i\kappa_\alpha \sin\vartheta$ on the left and right banks of $\Gamma_0$ respectively to get

$$-i\int_0^{i\infty + \frac{1}{2}\pi} \left(e^{-i\varpi\kappa_\alpha \cos(\theta - \vartheta)} + e^{-i\varpi\kappa_\alpha \cos(\theta + \vartheta)}\right) d\vartheta, \tag{10·2}$$

where $\vartheta$ takes the path from 0 to $\frac{1}{2}\pi$ and thence to $i\infty + \frac{1}{2}\pi$. In the first integrand of (10·2) write $\theta - \vartheta = iw$, and in the second $\theta + \vartheta = iw$, to obtain

$$-\int_C e^{-i\varpi\kappa_\alpha \cosh w} dw, \tag{10·3}$$

where $C$ starts from $-\infty + i(\frac{1}{2}\pi - \theta)$, runs parallel to the real axis to $i(\frac{1}{2}\pi - \theta)$, then runs down the imaginary axis to $i(-\frac{1}{2}\pi - \theta)$, and finally parallel to the real axis to $\infty + i(-\frac{1}{2}\pi - \theta)$. We now write $w = t + \frac{1}{2}i\pi$, and (10·3) becomes

$$-\int_{C'} e^{\kappa_\alpha \varpi \sinh t} dt, \tag{10·4}$$

where $C'$ is the path joining $(-\infty - i\theta, -i\theta, -i\theta - i\pi, \infty - i\theta - i\pi)$. Because $\varpi\kappa_\alpha$ is real and $\theta$ lies in the first quadrant, the end-points of the path $C'$ can be shifted to $-\infty$ and $\infty - i\pi$ without altering the value of the integral. But we have thus obtained a standard expression for $-\pi i Hi_0(\varpi\kappa_\alpha)$ (Copson 1935, p. 324), and (10·1) is proved.

If we now wish to find an approximation for the integral in (10·1) we can use the form (10·2) which shows that the first integrand has a saddle-point at $\vartheta = \theta$, while the second has none on the path of integration. We therefore evaluate at the one saddle-point, using Kelvin's method of stationary phase (Lamb 1932, p. 395), by which

$$\int_a^b \phi(x)\, e^{if(x)}\, dx = \sqrt{\left(\frac{2\pi}{|f''(x_0)|}\right)} \phi(x_0)\, e^{i[f(x_0) \pm \frac{1}{4}\pi]}, \tag{10·5}$$

approximately, provided $f'''(x_0)/[|f''(x_0)|]^{\frac{3}{2}}$ is small and $\phi(x)$ changes slowly compared with $e^{if(x)}$. Here $x_0$ is the saddle-point (point of stationary phase), and the upper or lower sign in the exponent is used according as $f''(x_0) \gtrless 0$. Applying this theorem to (7·11) we have

$$\phi_0 = \sqrt{\left(\frac{2\pi\alpha}{\varpi\omega}\right)} e^{i\omega(t - \varpi/\alpha) + \frac{3}{4}i\pi} \tag{10·6}$$

approximately, provided $\varpi\kappa_\alpha$ is large.

Since the exponent in $_p\phi_\alpha$ is identical with that in $\phi_0$ except for the sign of $z$, we can get an approximation by the same method. When we come to set down the value of the multiplier of the exponential at the saddle-point, we note that $\lambda_\beta$ must be positive imaginary on the upper edge of the cut, for the same reasons as given for $\lambda_\alpha$. Then we obtain, provided $\varpi'\kappa_\alpha$ is large,

$$_p\phi_\alpha \doteq 8 \sqrt{\left(\frac{2\pi\alpha}{\varpi'\omega}\right)} L(\theta)\, e^{i\omega(t-\varpi'/\alpha)+\frac{3}{4}i\pi}, \tag{10.7}$$

where $\quad L(\theta) = \dfrac{\cos^2\theta \sin\theta \sqrt{(\alpha^2/\beta^2-\cos^2\theta)}}{(\alpha^2/\beta^2-2\cos^2\theta)^2+4\cos^2\theta \sin\theta \sqrt{(\alpha^2/\beta^2-\cos^2\theta)}} \quad$ with $\quad \tan\theta = \dfrac{h+z}{x}$. (10.8)

To find the expression for the wave $PP$ we must combine (10.7) with $-\phi_r$ which is given approximately by

$$-\sqrt{\left(\frac{2\pi\alpha}{\varpi'\omega}\right)} e^{i\omega(t-\varpi'/\alpha)+\frac{3}{4}i\pi} \quad \text{when} \quad \varpi'\kappa_\alpha \text{ is large,} \tag{10.9}$$

analogous to (10.6). These two expressions cancel out (i.e. $PP$ changes phase) when

$$8L(\theta) = 1, \tag{10.10}$$

i.e. in the case $\lambda = \mu$, when

$$4\tan\theta \sqrt{(3\tan^2\theta+2)} = (3\tan^2\theta+1)^2. \tag{10.11}$$

This is identical with the result obtained by Jeffreys for plane harmonic waves (Jeffreys 1926 b), as it should be, since we have approximated at a particular value $\omega$ and a particular point $\zeta$.

Turning next to $_p\psi_\alpha$ (7.13), we make the same substitution, with the same rule for signs of $\lambda_\alpha$ and $\lambda_\beta$, and we see that when we consider the part of the contour which lies above the real axis, the exponent is

$$-i\kappa_\alpha[x\cos\vartheta+h\sin\vartheta+z\sqrt{(\alpha^2/\beta^2-\cos^2\vartheta)}]. \tag{10.12}$$

This is stationary when $\vartheta$ satisfies

$$x\sin\vartheta-h\cos\vartheta-\frac{z\cos\vartheta\sin\vartheta}{\sqrt{(\alpha^2/\beta^2-\cos^2\vartheta)}} = 0. \tag{10.13}$$

If $\vartheta_1$ is the root of (10.13), the time of arrival of the wave will be

$$t = \frac{1}{\alpha}[x\cos\vartheta_1+h\sin\vartheta_1+z\sqrt{(\alpha^2/\beta^2-\cos^2\vartheta_1)}]. \tag{10.14}$$

But (10.13) and (10.14) are reducible to the equations which determine $PS$ by the minimum-time principle.

It may be shown that there is no point of stationary phase on the contour below the real axis. Thus $_p\psi_\alpha$ evaluated by this method gives the wave $PS$, incident at the surface at the angle $\vartheta_1$ which is given by (10.13). Using this value of $\vartheta$ we can evaluate an approximation for $_p\psi_\alpha$ when $x\kappa_\alpha$ is large, corresponding to (10.7).

In this section, by consideration of the limit of the contour $\Gamma$ when $\omega$ lies on the positive real axis, we have been able to identify $_p\phi_\alpha$ and $_p\psi_\alpha$ as $PP$ and $PS$ respectively, obtaining accurate expressions for their travel times. In the same way we can identify other waves. But if we wish to generalize from waves to pulses we meet the difficulty that our approximations hold only as long as $\omega$ is large enough for the exponential factor in each integrand

to oscillate rapidly compared with changes in its multiplier. In generalizing from $e^{i\omega t}$, we therefore prefer to use a contour which avoids the neighbourhood of the origin. To do this we revert to the contours $\Gamma_\alpha$, $\Gamma_\beta$ and $\Gamma_\gamma$ for complex $\omega$, losing accuracy in our approximations to the travel-time and amplitude, but gaining the power to generalize more effectively.

## 11. DIRECT AND REFLECTED PULSES

We now evaluate $\phi_0$ by approximation on $\Gamma_\alpha$. We must consider the cases $\mathscr{R}(\omega) \gtrless 0$ separately.
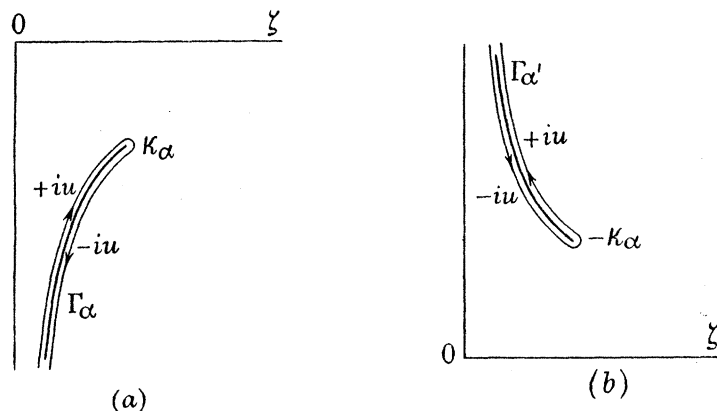


FIGURE 10. Evaluation along (a) $\Gamma_\alpha$ for $\mathscr{R}(\omega) > 0$, (b) $\Gamma_\alpha'$ for $\mathscr{R}(\omega) < 0$.

(a)  $\mathscr{R}(\omega) > 0$

By (7·11)
$$\phi_0 = -\int_{\Gamma_\alpha} e^{-i\zeta x - (h-z)\lambda_\alpha} \frac{d\zeta}{\lambda_\alpha} e^{i\omega t} \quad \text{when} \quad \mathscr{R}(\omega) > 0.$$

If $\Gamma_\alpha$ lies indefinitely near to the cut $\mathscr{R}(\lambda_\alpha) = 0$, we may write $\lambda_\alpha = \pm iu$ on $\Gamma_\alpha$, where $u$ is real and positive. The positive sign will refer to one side of the cut, and the negative sign to the other. The easiest way to determine which sign is positive is to write $\zeta = p\kappa_\alpha$, and consider the cases $p \gtrless 1$. The facts that $\kappa_\alpha = (s - ic)/\alpha$, and $\mathscr{R}(\lambda_\alpha)$ must be positive, lead to the conclusion that $\mathscr{I}(\lambda_\alpha)$ must be positive on the left of the cut, and negative on the right, as in figure 10 a. Then since $\zeta = \sqrt{(\kappa_\alpha^2 - u^2)}$, $\zeta \, d\zeta = -u \, du$, we get

$$\phi_0 = i \int_0^\infty e^{-ix\zeta} \left[ e^{-(h-z)iu} + e^{(h-z)iu} \right] \frac{du}{\zeta} e^{i\omega t}. \tag{11·1}$$

Approximating to $\zeta$ in the denominator by $\kappa_\alpha$, and in the exponent by $\kappa_\alpha - u^2/2\kappa_\alpha$,

$$\phi_0 \doteqdot \frac{2i}{\kappa_\alpha} e^{i\omega t - ix\kappa_\alpha} \int_0^\infty e^{ixu^2/2\kappa_\alpha} \cos (h-z)\, u \, du \tag{11·2}$$

$$= \sqrt{\left( \frac{2\pi\alpha i^3}{x\omega} \right)} \exp\left[ i\omega \left\{ t - \frac{1}{\alpha} \left[ x + \frac{(h-z)^2}{2x} \right] \right\} \right], \tag{11·3}$$

provided $|x\kappa_\alpha|$ is large and $\mathscr{I}(\kappa_\alpha) < 0$. \tag{11·4}

(b)  $\mathscr{R}(\omega) < 0$

Here
$$\phi_0 = -\int_{\Gamma_\alpha'} e^{i\zeta x - (h-z)\lambda_\alpha} \frac{d\zeta}{\lambda_\alpha} e^{i\omega t}, \quad \mathscr{R}(\omega) < 0$$

and the contour $\Gamma_\alpha'$ has the form shown in figure 10 b. We find that $\mathscr{I}(\lambda_\alpha)$ must be negative on the left of the cut and positive on the right, and with the same substitutions as before

except for signs, we obtain exactly the same expression $(11\cdot1)$ as before. Thus $(11\cdot3)$ holds for all $\omega$ not too near the origin and such that $\mathscr{I}(\omega)<0$. This is the response to $e^{i\omega t}$. Then the response to $H(t)$ when $(h-z)/x$ is small will be

$$\Phi_0 \doteqdot \sqrt{\left(\frac{2\pi\alpha i^3}{x}\right)}\frac{1}{2\pi i}\int_\Omega \omega^{-\frac{3}{2}}e^{i\omega\tau}\,d\omega, \quad \text{where} \quad \tau = t-\frac{1}{\alpha}\left[x+\frac{(h-z)^2}{2x}\right] \tag{11·5}$$

$$= -2\sqrt{\left(\frac{2\alpha\tau}{x}\right)}H(\tau) \tag{11·6}$$

by use of $(2\cdot3)$. In this case we can use the approximation $(11\cdot3)$ which is not valid in the neighbourhood of the origin in the $\omega$-plane, since the contour $\Omega$ can be taken as any line below the real axis from $-\infty-ic$ to $\infty-ic$. We may compare our expression for $\Phi_0$ $(11\cdot6)$ with the accurate result $(4\cdot6)$

$$\Phi_0 = -2\cosh^{-1}\frac{\alpha t}{\varpi}H\left(t-\frac{\varpi}{\alpha}\right). \tag{11·7}$$

$\tau$ in $(11\cdot6)$ will be a good approximation to $t-\varpi/\alpha$ in $(11\cdot7)$ if $x$ is large compared with $h$ and $z$. Writing $t-\varpi/\alpha = \tau_0$ in $(11\cdot7)$ we get

$$\Phi_0 = -4\left[\left(\frac{\alpha\tau_0}{2\varpi}\right)^{\frac{1}{2}}-\frac{1}{6}\left(\frac{\alpha\tau_0}{2\varpi}\right)^{\frac{3}{2}}+O\left(\frac{\alpha\tau_0}{2\varpi}\right)^{\frac{5}{2}}\right]H(\tau_0). \tag{11·8}$$

$(11\cdot6)$ will be a good approximation to $(11\cdot8)$ if $|h-z|/x$ is small and also if $\alpha\tau_0/2\varpi$ is small, i.e. at the onset of the disturbance.

The displacements derived from $\Phi_0$ as given by $(11\cdot6)$ are

$$U(\Phi_0) = \frac{\partial\Phi_0}{\partial\kappa} \doteqdot \sqrt{\left(\frac{2}{x\alpha\tau}\right)}H(\tau), \tag{11·9}$$

$$W(\Phi_0) = \frac{\partial\Phi_0}{\partial z} \doteqdot -\frac{(h-z)}{x}\sqrt{\left(\frac{2}{x\alpha\tau}\right)}H(\tau). \tag{11·10}$$

We notice that these tend to zero as $\tau$ tends to infinity, so that our approximation fails to record any residual displacement.

Next consider

$$_p\phi_\alpha = \int_{\Gamma_\alpha}\frac{8\zeta^2\lambda_\beta}{F(\zeta)}e^{-ix\zeta-(h+z)\lambda_\alpha}\,d\zeta\,e^{i\omega t}. \tag{11·11}$$

Since we are taking $\omega$ large enough for the exponent to vary much faster than the remainder of the integrand, we take

$$\lambda_\beta = \sqrt{(\zeta^2-\kappa_\beta^2)} = i\sqrt{[(\kappa_\beta^2-\kappa_\alpha^2)+u^2]} \doteqdot i\kappa_1, \tag{11·12}$$

thus defining $\kappa_1 = \sqrt{(\kappa_\beta^2-\kappa_\alpha^2)}$, and

$$F(\zeta) \doteqdot (2\zeta^2-\kappa_\beta^2)^2 \doteqdot (\kappa_\beta^2-2\kappa_\alpha^2)^2 = \kappa_2^4, \tag{11·13}$$

defining $\kappa_2$. We shall also use the additional symbols $\beta_1$ and $\beta_2$ defined by

$$\beta_1^{-2} = \beta^{-2}-\alpha^{-2}, \quad \beta_2^{-2} = \beta^{-2}-2\alpha^{-2}. \tag{11·14}$$

$\beta_1$ and $\beta_2$ have the dimensions of velocity, and in the Poisson case

$$\beta_1 = \sqrt{\tfrac{3}{2}}\beta, \quad \beta_2 = \sqrt{3}\beta = \alpha.$$

Evaluating as before we get, provided $(h+z)/x$ is small,

$$_p\Phi_\alpha \doteqdot -16\sqrt{\left(\frac{2\alpha\tau}{x}\right)}\frac{\beta_2^4}{\alpha^3\beta_1}\frac{(h+z)}{x}H(\tau), \tag{11.15}$$

where $\tau$ is now given by

$$\tau = t - \frac{1}{\alpha}[x+(h+z)^2/2x]. \tag{11.16}$$

The complete expression for $PP$ is derived by combining (11.15) with

$$-\Phi_r \doteqdot 2\sqrt{\left(\frac{2\alpha\tau}{x}\right)}H(\tau). \tag{11.17}$$

From (11.15) and (11.17) we see that at very large distances $_p\Phi_\alpha$ is negligible compared with $-\Phi_r$, but owing to the large numerical factor in the ratio

$$_p\Phi_\alpha/(-\Phi_r) = -8\frac{\beta_2^4}{\alpha^3\beta_1}\frac{h+z}{x}$$

$(= 8\sqrt{2}\,(h+z)/x$ in the Poisson case), reversal of phase takes place for a small angle of incident ray. Our approximation gives the critical value of $(h+z)/x$ as $\sqrt{2}/16 = 0.0884$ which is a poor approximation to the true value of $0.2270$ given by (10.11), and shows that our approximations begin to break down at such short distances, because the Sommerfeld loop is too far from the saddle-point.

Comparing (11.15) and (11.17) with (11.6) we see that the form of the reflected pulse is essentially the same as that of the direct pulse—a sharp kick followed by an infinitely protracted recovery.

In the same way we find, when $(h+z)/x$ is small,

$$_p\Psi_\alpha \doteqdot -8\sqrt{\left(\frac{2\alpha\tau}{x}\right)}\frac{h\beta_2^2}{x\alpha^2}(1-\beta_1 z/\alpha x)^{-\frac{3}{2}}H(\tau), \tag{11.18}$$

where

$$\tau = t - x/\alpha - z/\beta_1 - h^2/2(\alpha x - \beta_1 z). \tag{11.19}$$

Thus the pulse $PS$ is of the same type as the initial pulse, but falls off faster with increasing distance.

We now turn to the disturbance due to initial $S$-pulse, and derive the expressions for the direct pulse, $SS$, and $SP$.

$\psi_0$ of (7.14) is identical with $\phi_0$ of (7.11) except that $\beta$ replaces $\alpha$. We can therefore write down the approximations which would be obtained from the loop $\Gamma_\beta$, valid when $|h-z|/x$ and $\beta\tau/x$ are small:

$$\Psi_0 \doteqdot -2\sqrt{\left(\frac{2\beta\tau}{x}\right)}H(\tau), \quad \text{where} \quad \tau = t-\frac{1}{\beta}\left[x+\frac{(h-z)^2}{2x}\right], \tag{11.20}$$

and by (3.3),

$$U(\Psi_0) \doteqdot -\frac{h-z}{x}\sqrt{\left(\frac{2}{\beta x\tau}\right)}H(\tau), \tag{11.21}$$

$$W(\Psi_0) \doteqdot -\sqrt{\left(\frac{2}{\beta x\tau}\right)}H(\tau). \tag{11.22}$$

An equal and opposite pulse from the image source would give

$$-\Psi_r \doteqdot 2\sqrt{\left(\frac{2\beta\tau}{x}\right)}H(\tau), \quad \text{where} \quad \tau = t-\frac{1}{\beta}\left[x+\frac{(h+z)^2}{2x}\right], \tag{11.23}$$

when $(h+z)/x$ and $\beta\tau/x$ are small. The reflected pulse $SS$ will be compounded of this and $_s\Psi_\beta$. When $\mathscr{R}(\omega)>0$,

$$_s\psi_\beta = \int_{\Gamma_\beta} \frac{8\zeta^2\lambda_\alpha}{F(\zeta)}\, e^{-i\zeta x-(h+z)\lambda_\beta}\, d\zeta\, e^{i\omega t}. \tag{11.24}$$

Just as for $\Gamma_\alpha$, we write $\lambda_\beta = +iv$ on the left side of $\Gamma_\beta$, $\lambda_\beta = -iv$ on the right. Then

$$\zeta = \sqrt{(\kappa_\beta^2-v^2)} \doteq \kappa_\beta(1-v^2/2\kappa_\beta^2), \quad \lambda_\alpha = +\kappa_1, \quad \zeta d\zeta = -v\, dv \quad \text{and} \quad F(\zeta) \doteq \kappa_\beta^4.$$

Thus

$$_s\psi_\beta \doteq 8\sqrt{\left(\frac{2\pi\beta i^3}{x\omega}\right)}\frac{\beta}{\beta_1}\frac{h+z}{x}\, e^{i\omega\tau-\frac{1}{4}i\pi}, \tag{11.25}$$

when $(h+z)/x$ is small, and $\tau$ is given by $(11.23)$.

When $\mathscr{R}(\omega)<0$,

$$_s\psi_\beta = \int_{\Gamma_\beta'} \frac{8\zeta^2\lambda_\alpha}{F(\zeta)}\, e^{i\zeta x-(h+z)\lambda_\beta}\, d\zeta\, e^{i\omega t}.$$

$\lambda_\beta = -iv$ on the left of $\Gamma_\beta'$ and $\lambda_\beta = +iv$ on the right,

$$\zeta = \sqrt{(\kappa_\beta^2-v^2)} \doteq -\kappa_\beta(1-v^2/2\kappa_\beta^2) \quad \text{and} \quad \lambda_\alpha \doteq -\kappa_1.$$

Making these substitutions, and evaluating as usual, we get

$$_s\psi_\beta \doteq 8\sqrt{\left(\frac{2\pi\beta i^3}{x\omega}\right)}\frac{\beta}{\beta_1}\frac{h+z}{x}\, e^{i\omega\tau+\frac{1}{4}i\pi}. \tag{11.26}$$

Thus

$$_s\psi_\beta \doteq Ai^{\frac{3}{2}}\omega^{-\frac{1}{2}}\, e^{i\omega\tau\pm\frac{1}{4}i\pi} \quad \text{according as } \mathscr{R}(\omega) \lessgtr 0, \tag{11.27}$$

where

$$A = 8\sqrt{\left(\frac{2\pi\beta}{x}\right)}\frac{\beta}{\beta_1}\frac{h+z}{x}. \tag{11.28}$$

Considering now the two parts of $SS$ for given $\omega$, we see that the amplitudes are in the ratio $|\,_s\psi_\beta\,|/|\,\psi_r\,| = 8\beta(h+z)/\beta_1 x$, which is small when $(h+z)/x$ is small. The phase of $_s\psi_\beta$ exceeds that of $-\psi_r$ by $\pm\frac{1}{2}\pi$ according as $\mathscr{R}(\omega) \lessgtr 0$, so that the amplitude of the sum of $-\psi_r$ and $_s\psi_\beta$ differs from $|\,\psi_r\,|$ by a small quantity of the second order if $(h+z)/x$ is first order. This corresponds to the fact that with plane waves for angles near grazing incidence no energy goes into $SP$, $SS$ being reflected with unchanged amplitude but changed phase (Jeffreys 1926 b).

The above evaluation of $_s\psi_\beta$ differs in one important respect from previous approximations on $\Gamma_\alpha$. Whereas approximations obtained from $\Gamma_\alpha$ hold (subject to the conditions stated) as $\omega$ approaches and crosses the imaginary axis of $\omega$, $(11.27)$ holds only as long as $\Gamma_\beta$ is not too near $\Gamma_\alpha$. If $\Gamma_\beta$ lies so near to $\Gamma_\alpha$ that contributions to the contour integral in the neighbourhood of $\kappa_\beta$ from $\Gamma_\alpha$ have to be taken into account, $(11.27)$ breaks down. The same condition holds near $-\kappa_\beta$ when $\mathscr{R}(\omega)<0$. In other words, $(11.27)$ holds only as long as $\arg\omega$ lies outside $-\frac{1}{2}\pi\pm\epsilon$, where $\epsilon$ is a small angle determined by the nature of the integrand in $(11.24)$. Across this small sector there takes place a continuous transition between the two expressions given in $(11.27)$. We therefore obtain the response to $H(t)$ as described in §2, replacing $\Omega$ by $\Omega'$ and using the time derivative to avoid encountering a singularity at the origin,

$$_s\dot\Psi_\beta \doteq -\frac{A}{\pi}\int_0^\infty \omega^{-\frac{1}{2}}\sin\left(\omega\tau-\tfrac{1}{4}\pi\right)d\omega \tag{11.29}$$

$$= \frac{A}{\pi}\int_0^\infty \omega^{-\frac{1}{2}}\sin\left(\omega\tau'+\tfrac{1}{4}\pi\right)d\omega, \quad \text{writing } \tau'=-\tau,$$

$$= 8\sqrt{\left(\frac{2\beta}{x\tau'}\right)}\frac{\beta}{\beta_1}\frac{h+z}{x}\, H(\tau'). \tag{11.30}$$

This approximation differs from that for $\dot{\Psi}_0'$ only in numerical coefficients and in the occurrence of $\sin(\omega\tau - \frac{1}{4}\pi)$ in (11·29), where $\dot{\Psi}_0'$ has $\sin(\omega\tau - \frac{1}{4}\pi)$; it is this difference which distorts the shape of the pulse.*
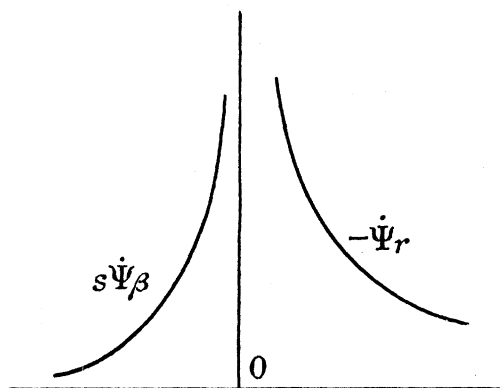


FIGURE 11. $_s\dot{\Psi}_\beta$ and $-\dot{\Psi}_r$ as functions of $\tau$.

$_s\dot{\Psi}_\beta$ and $-\dot{\Psi}_r$ are graphed against $\tau$ in figure 11. Since $w = -\partial\Psi/\partial x \doteq \dot{\Psi}/\beta$, this figure shows the form of the vertical displacement. It is clear that $_s\Psi_\beta$ does not modify the amplitude of the disturbance due to $-\Psi_r'$, since that lies entirely subsequent to the instant $\tau = 0$, whereas $_s\Psi_\beta$ gives a disturbance preceding $\tau = 0$. The effect of the term $_s\Psi_\beta$ is therefore to lead up to the jerk given by $-\Psi_r'$, and its relative size decreases with distance from the epicentre.

The evaluation of $_s\Phi_\alpha$ is exactly analogous to that of $_p\Psi_\alpha$, and the result is, when $(h+z)/x$ is small,

$$_s\Phi_\alpha \doteq 8\sqrt{\left(\frac{2\alpha\tau}{x}\right)} \frac{z}{x}\frac{\beta_2^2}{\alpha^2}\left(1 - \frac{h\beta_1}{xa}\right)^{-\frac{3}{2}} H(\tau), \tag{11·31}$$

where

$$\tau = t - \left[\frac{x}{\alpha} + \frac{h}{\beta_1} + \frac{z^2}{2(\alpha x - \beta_1 h)}\right]. \tag{11·32}$$

This is $SP$, and its properties can be derived from those of $PS$ by change of sign and interchange of $h$ and $z$, as long as $z \neq 0$. If $z = 0$, the approximation given in (11·31) vanishes, and we must consider the contribution from terms which can be neglected as long as $z \neq 0$.

## 12. RAYLEIGH-PULSES

The contributions from the loop $\Gamma_\gamma$ can be evaluated exactly, since $\kappa_\gamma$ is not a branch-point but a pole. When $\zeta = \kappa_\gamma$,

$$\lambda_\alpha = \sqrt{(\zeta^2 - \kappa_\alpha^2)} = \omega/\gamma_\alpha, \quad \text{where} \quad \gamma_\alpha^{-2} = \gamma^{-2} - \alpha^{-2}, \tag{12·1}$$

$$\lambda_\beta = \sqrt{(\zeta^2 - \kappa_\beta^2)} = \omega/\gamma_\beta, \quad \text{where} \quad \gamma_\beta^{-2} = \gamma^{-2} - \beta^{-2}, \tag{12·2}$$

the positive signs being taken before the radicals, since $\kappa_\gamma$ is on the top sheet of the Riemann surface and $\mathscr{R}(\omega) > 0$. Then, evaluating the residue at $\kappa_\gamma$, we obtain, for $\mathscr{R}(\omega) > 0$,

$$_p\phi_\gamma = 8\int_{\Gamma_\gamma} \frac{\zeta^2\lambda_\beta}{F(\zeta)} e^{-i\zeta x - (h+z)\lambda_\alpha} d\zeta\, e^{i\omega t}$$

$$= A_r i\, e^{-p\omega + i\omega\tau}, \tag{12·3}$$

* The same phenomenon occurs in the horizontal displacement at time $x/\beta$ in Lamb's problem (1904, p. 21 and figure 4).

where
$$A_r = -\frac{16\pi}{\gamma^2\gamma_\beta}\frac{\omega^3}{F'(\kappa_\gamma)} = 4\pi\gamma\gamma_\alpha(\gamma_\alpha^2+\gamma_\beta^2+2\gamma^2-4\gamma_\alpha\gamma_\beta+2\gamma^2\gamma_\alpha\gamma_\beta/\beta^2)^{-1}, \tag{12·4}$$

$$p = (h+z)/\gamma_\alpha \quad \text{and} \quad \tau = t-x/\gamma. \tag{12·5}$$

$A_r$ is a real constant.

If, on the other hand, we consider $\mathscr{R}(\omega)<0$, we must choose the negative signs for $\lambda_\alpha$ and $\lambda_\beta$, and note that the pole is now at $-\kappa_\gamma$ and is encircled in the reverse direction by $\Gamma'_\gamma$. In place of (12·3) we obtain

$$_p\phi_\gamma = -A_r i\,e^{+p\omega+i\omega\tau}. \tag{12·6}$$

(12·3) and (12·6) are adequate expressions for the Rayleigh-wave provided $\kappa_\gamma$ is not so close to $\Gamma_\alpha$ and $\Gamma_\beta$ that the integrals along those loops make significant contributions in the neighbourhood of the pole $\kappa_\gamma$, and similarly for $-\kappa_\gamma$, $\Gamma'_\alpha$ and $\Gamma'_\beta$. That is, (12·3) and (12·6) hold except within the sector $\arg\omega = -\frac{1}{2}\pi\pm\epsilon$ ($\epsilon$ being small), across which there is a rapid but continuous transition from (12·3) to (12·6). We therefore obtain the response to $H(t)$ from the contour $\Omega'$, using displacements, which are

$$\left.\begin{array}{l} u = \mp\dfrac{A_r\omega}{\gamma}e^{\pm p\omega+i\omega\tau} \\[2mm] w = -\dfrac{A_r i\omega}{\gamma_\alpha}e^{\pm p\omega+i\omega\tau} \end{array}\right\} \quad \text{according as } \mathscr{R}(\omega)\lessgtr 0.$$

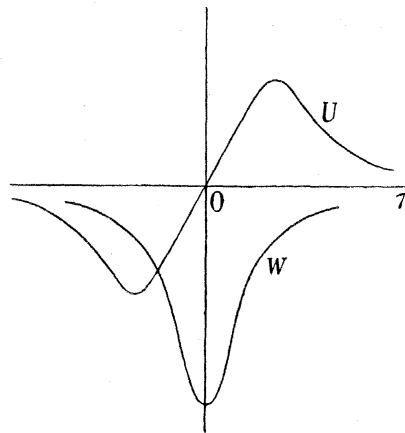$$\tag{12·7}$$

$$\tag{12·8}$$



FIGURE 12. $U$ and $W$ for the Rayleigh-pulse $_p\Phi_\gamma$ as functions of $\tau$.

Using (2·8) and (2·7) respectively, we find the displacements corresponding to initial unit-pulse

$$U = \frac{A_r}{\pi\gamma}\frac{\tau}{p^2+\tau^2}, \tag{12·9}$$

$$W = -\frac{A_r}{\pi\gamma_\alpha}\frac{p}{p^2+\tau^2}. \tag{12·10}$$

$U$ and $W$ are graphed against $\tau$ in figure 12. In each curve, the greatest displacement is inversely proportional to $p = (h+z)/\gamma_\alpha$. Thus (12·9) and (12·10) represent a pulse confined to the neighbourhood of the surface, travelling with velocity $\gamma$, and whose sharpness decreases

with increasing depth of focus. This is the Rayleigh-pulse, of which $_p\Phi_\gamma$ gives the irrotational part. The distortional part, given by $_p\Psi_\gamma$, is found in exactly the same way to be

$$U = -\frac{A'_r}{\pi\gamma_\beta}\frac{\tau}{p'^2+\tau^2}, \tag{12.11}$$

$$W = \frac{A'_r}{\pi\gamma}\frac{p'}{p'^2+\tau^2}, \tag{12.12}$$

where        $A'_r = \frac{1}{2}\gamma\gamma_\beta\left(\frac{2}{\gamma^2}-\frac{1}{\beta^2}\right)A_r$,   $p' = h/\gamma_\alpha + z/\gamma_\beta$   and   $\tau = t - x/\gamma$.

The amplitude of the Rayleigh-pulse contains no $x$-factor. So in this two-dimensional case, frictional loss being neglected, the pulse travels along the surface with undiminishing amplitude.

When the initial disturbance is an $S$-pulse, the displacements in the Rayleigh-pulse are

$$U = \frac{A'_r}{\pi\gamma}\frac{q'}{q'^2+\tau^2} - \frac{A_r}{\pi\gamma_\alpha}\frac{q}{q^2+\tau^2}, \tag{12.13}$$

$$W = \frac{A'_r}{\pi\gamma_\alpha}\frac{\tau}{q'^2+\tau^2} - \frac{A_r\gamma_\beta}{\pi\gamma\gamma_\alpha}\frac{\tau}{q^2+\tau^2}, \tag{12.14}$$

where $q = (h+z)/\gamma_\beta$, $q' = h/\gamma_\beta + z/\gamma_\alpha$.

### 13. The surface $P$-pulse

So far we have dealt with the features of the disturbance which are geometrically evident and with the Rayleigh-pulse. We now consider the four remaining integrals, $_s\psi_\alpha$, $_p\phi_\beta$, $_p\psi_\beta$ and $_s\phi_\beta$, whose contribution to the disturbance, if any, is certainly not evident from the geometry of reflexion. In this section we deal with $_s\psi_\alpha$, since the mathematical treatment follows methods already developed in §11.

By evaluation on $\Gamma_\alpha$ as before we obtain, when $(h+z)/x$ is small,

$$_s\Psi_\alpha \doteq \frac{32}{3}\sqrt{\left(\frac{2\alpha}{x}\right)}\frac{\beta_2^4}{\alpha^3 x}\left[1-\frac{(h+z)\beta_1}{\alpha x}\right]^{-\frac{3}{2}}\tau^{\frac{3}{2}}H(\tau), \tag{13.1}$$

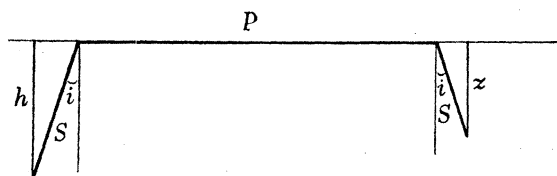where        $\tau = t - x/\alpha - (h+z)/\beta_1$. \tag{13.2}



FIGURE 13. Suggested path of $_s\Psi_\alpha$.

The result (13.1) differs from the formulae for $PP$, $PS$, etc., mainly in the occurrence of $\tau^{\frac{3}{2}}$ in place of $\tau^{\frac{1}{2}}$. It represents a pulse which started and finished as $S$, but travelled most of the way at the surface with velocity $\alpha$. It can therefore suitably be called the 'surface $P$-pulse'. The value of $\tau$ given in (13.2) corresponds exactly to that of a ray which travelled as shown in figure 13, with angles of incidence and emergence $i = \sin^{-1}(\beta/\alpha)$.

If $x/(h+z)$ is large, the displacements are given by

$$U \doteq -16 \sqrt{\left(\frac{2\alpha}{x}\right)} \frac{\beta_2^4}{\alpha^3 \beta_1 x} \tau^{\frac{1}{2}}, \tag{13.3}$$

$$W \doteq 16 \sqrt{\left(\frac{2\alpha}{x}\right)} \frac{\beta_2^4}{\alpha^4 x} \tau^{\frac{1}{2}}. \tag{13.4}$$

Thus the displacements of the surface $P$-pulse have the same form as the potentials of the reflected pulses, and consequently, to a first approximation, the velocities of the surface $P$-pulse have the same form as the displacements for the reflected pulses, i.e. the disturbance begins not with a sudden jerk, but with a suddenly acquired great velocity, the initial displacement being zero.

It is easily verified that the path shown in figure 13 is a minimum-time path. Moreover, the magnitude of the disturbance at the point of reception does not decrease as $h$ and $z$ increase, i.e. the disturbance is not confined to the neighbourhood of the surface. Thus the surface $P$-pulse is not a surface effect analogous to the Rayleigh-pulse, but more of the same nature as the ordinary reflected pulses. This distinguishes it from the surface $S$-pulse, next to be considered, which can only be discerned near the surface, like the Rayleigh-pulse, and has not a minimum-time path.

## 14. THE SURFACE $S$-PULSE

Transforming $_p\phi_\beta$ in (7.12) by the usual substitutions on $\Gamma_\beta$ we get, when $\mathscr{R}(\omega)>0$, provided $|x\omega/\beta|$ and $x/(h+z)$ are large,

$$_p\phi_\beta = 16i \int_0^\infty \frac{(\kappa_\beta^2 - 2v^2)^2 \sqrt{(\kappa_\beta^2 - v^2)}\, v^2\, dv}{(\kappa_\beta^2 - 2v^2)^4 + 16v^2(\kappa_\beta^2 - v^2)^2 (\kappa_1^2 - v^2)} e^{-ix\sqrt{(\kappa_\beta^2 - v^2)} - (h+z)\sqrt{(\kappa_1^2 - v^2)} + i\omega t} \tag{14.1}$$

$$\doteq \frac{16i}{\kappa_\beta^3} e^{i\omega\tau - \omega p} \int_0^\infty e^{ixv^2/2\kappa_\beta} v^2\, dv$$

$$= B\sqrt{\pi}\, i^{\frac{3}{2}} \omega^{-\frac{3}{2}} e^{i\omega\tau - \omega p}, \tag{14.2}$$

where $\tau = t - x/\beta$, $p = (h+z)/\beta_1$ and $B = 8\sqrt{2}\beta^{\frac{3}{2}}x^{-\frac{3}{2}}$. Similarly, evaluating on $\Gamma_\beta'$ for $\mathscr{R}(\omega)<0$,

$$_p\phi_\beta \doteq B\sqrt{\pi}\, i^{\frac{3}{2}} \omega^{-\frac{3}{2}} e^{i\omega\tau + p\omega}. \tag{14.3}$$

This response is a surface wave, with amplitude diminishing downwards as $e^{-(h+z)\omega/\beta_1}$. The phase retardation is $x/\beta$.

As with all other approximations from $\Gamma_\beta$, (14.2) and (14.3) cease to hold if $\Gamma_\alpha$ passes too close to $\kappa_\beta$, or $\Gamma_\alpha'$ too close to $-\kappa_\beta$, and so here we find the response to $H(t)$ from $\Omega'$, again choosing the integrand so as to ensure convergence at the origin.

We therefore examine the velocity

$$\dot{u} \doteq -\frac{B\sqrt{\pi}}{\beta} i^{\frac{1}{2}} \omega^{\frac{1}{2}} e^{i\omega\tau \pm \omega p} \quad \text{as} \quad \mathscr{R}(\omega) \lessgtr 0. \tag{14.4}$$

From this, under certain conditions specified below, we can derive

$$\dot{U} = \frac{1}{2\pi i} \int_{\Omega'} \dot{u}\, \frac{d\omega}{\omega}$$

$$\doteq -\frac{B}{\beta} p^{-\frac{1}{2}} \cos^{\frac{1}{2}}\psi \sin\left(\tfrac{1}{2}\psi + \tfrac{1}{4}\pi\right), \quad \text{where} \quad \tan\psi = \frac{\tau}{p}, \tag{14.5}$$

by (2.9). $\dot{U}$ varies with $\tau$ as shown in figure 14.

The condition for the approximation (14·2) to be valid is that $|x\omega/\beta|$ and $x/(h+z)$ shall be large. Thus the lower limit of $|\omega|$ for which it may be used decreases as $x$ increases. The derivation of (14·5) from (14·4), on the other hand, is exact, and so (14·5) will apply provided the integral from which it is derived receives a negligible contribution from those small values of $|\omega|$ for which (14·2) breaks down. It may be shown that the proportion contributed to the integral from such values diminishes as $p$ and $\tau$ decrease.

Thus we may show qualitatively that our approximation (14·5) for $\dot{U}$ may be expected to hold provided $x$ is large, $h$ and $z$ are small, and $\tau$ is small enough. Under these conditions, the surface $S$-pulse makes its arrival known at $t = z/\beta$ by a peak in the horizontal velocity, the sharpness of which increases with the shallowness of focus and reception point. The horizontal displacement will start gradually.
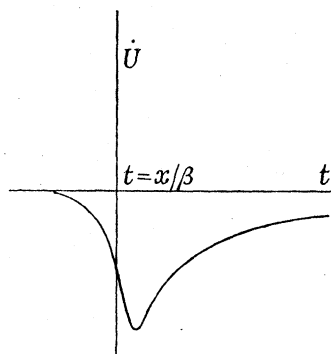


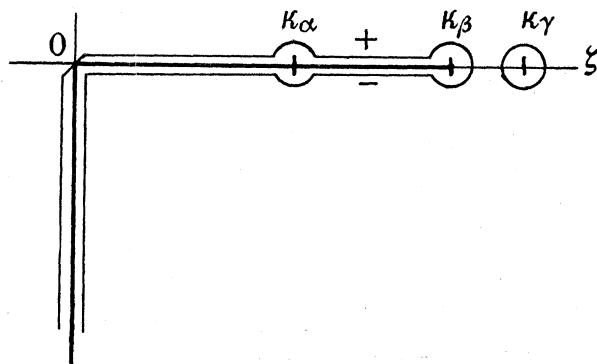FIGURE 14. $\dot{U}$ (for $pSp$) from approximation on $\Gamma_\beta$.



FIGURE 15. Limiting form of loop $\Gamma$ when $\omega$ is real and positive.

In order to remove some of the uncertainty of this result, we are driven to the procedure—hitherto avoided—of integrating first with regard to $\omega$. To do so, we must disentangle $\omega$ from the other variables in the integrand of (14·1), and this is feasible only for real $\omega$.

We therefore return to the limiting form of $\Gamma$ for $\omega$ real and $>0$. We have proved in § 10 that the neighbourhood of $\kappa_\alpha$ provides expressions for the reflected pulses (from initial $P$-pulse), and we are now concerned with the contribution from the loop which runs from $\kappa_\alpha$ around $\kappa_\beta$ (see figure 15). In the region of this loop, which we denote by $\Gamma_{\beta_0}$, all quantities in the integrand of (14·1) are single-valued except $\lambda_\beta$ and consequently $F(\zeta)$. It we write $\zeta = \kappa_\beta \cos\phi$, we find in the usual way that $\lambda_\beta$ takes the value $+i\kappa_\beta \sin\phi$ on the loop above the axis, and $-i\kappa_\beta \sin\phi$ below.

To avoid questions of convergence of the integral for $\omega$, we deal with

$$u = -8i \int_{\Gamma_{\beta_0}} \frac{\zeta^3 \lambda_\beta}{F(\zeta)} e^{-ix\zeta - (h+z)\lambda_\alpha + i\omega t} d\zeta$$

$$= -8i \int_0^{\cos^{-1}\beta/\alpha} \zeta^3 e^{-ix\zeta - (h+z)\lambda_\alpha + i\omega t} d\zeta \left( -\frac{i\kappa_\beta \sin\phi}{F_+} + \frac{-i\kappa_\beta \sin\phi}{F_-} \right)$$

$$= \frac{16\omega}{\beta} \int_0^{\cos^{-1}\beta/\alpha} \frac{(2\cos^2\phi - 1)^2 \cos^3\phi \sin^2\phi \, d\phi}{(2\cos^2\phi - 1)^4 + 16\cos^4\phi \sin^2\phi (\cos^2\phi - \beta^2/\alpha^2)} e^{i\omega T - \omega P}, \qquad (14\cdot6)$$

where
$$T = t - x\cos\phi/\beta, \quad P = (h+z)\sqrt{(\cos^2\phi - \beta^2/\alpha^2)}/\beta \qquad (14\cdot7)$$

and $F_+$ and $F_-$ denote the values of $F(\zeta)$ on the upper and lower sides of the loop. Writing $\cos\phi = w$, we get

$$u = \frac{16\omega}{\beta} \int_{\beta/\alpha}^1 G(w) e^{i\omega T - \omega P} dw, \qquad (14\cdot8)$$

with
$$G(w) = \frac{w^3 (2w^2 - 1)^2 \sqrt{(1 - w^2)}}{(2w^2 - 1)^4 + 16w^4 (1 - w^2)(w^2 - \beta^2/\alpha^2)},$$

$$T(w) = t - wx/\beta \quad \text{and} \quad P(w) = (h+z)\sqrt{(w^2 - \beta^2/\alpha^2)}/\beta. \qquad (14\cdot9)$$

When $\omega$ is negative, we use the appropriate signs and obtain the same result $(14\cdot8)$, except that the sign of $\omega P$ in the exponent becomes positive.

In this case, $\Omega'$ degenerates into the real axis, and we find that the response to initial unit pulse is

$$U = \frac{16}{\beta} \int_{\beta/\alpha}^1 G(w) \, dw \, \frac{1}{2\pi i} \int_{\Omega'} \omega e^{i\omega T \pm \omega P} \frac{d\omega}{\omega}$$

$$= \frac{16}{\pi\beta} \int_{\beta/\alpha}^1 G(w) \, dw \int_0^\infty e^{-\omega P} \sin\omega T \, d\omega$$

$$= \frac{16}{\pi} \int_{\beta/\alpha}^1 G(w) E(w) \, dw, \qquad (14\cdot10)$$

where
$$E(w) = \frac{1}{\beta} \frac{T}{P^2 + T^2}$$

$$= \frac{(\beta t - wx)}{(h+z)^2 (w^2 - \beta^2/\alpha^2) + (\beta t - wx)^2}. \qquad (14\cdot11)$$

$(14\cdot10)$ gives $U$ as a function of $x$, $h$, $z$ and $t$, but a long series of numerical integrations would be needed to obtain a close approximation to the true relationship. The shape of the factor $E(w)$, however, gives us a method of investigating qualitatively the variation of $U$ with $t$, when $(h+z)/x$ is small.

Given $t$, $E(w)$ has a single zero at $w = \beta t/x$, and at large distances from this zero it behaves like $(\beta t - wx)^{-1}$. In the immediate neighbourhood of the zero there are maximum and minimum at

$$w = \frac{\beta t}{x} \mp \frac{\beta(h+z)}{x} \sqrt{\frac{t^2 - x^2/\alpha^2}{x^2 + (h+z)^2}}, \qquad (14\cdot12)$$

respectively. When $(h+z)/x$ is small, and $t$ is not very different from $x/\beta$, $(14\cdot12)$ reduces to

$$\beta t/x \mp \beta(h+z)/\beta_1 x, \qquad (14\cdot13)$$

and the values of the maximum and minimum are

$$\pm \beta_1/2\beta(h+z). \qquad (14\cdot14)$$

From (14·13) and (14·14) we see that the peak and trough near the zero of $E(w)$ become very sharp when $(h+z)/x$ is very small; moreover, $E(w)$ is nearly zero everywhere except in this region. Thus, since $U$ is obtained by integrating the product of the ordinates of $G(w)$ and $E(w)$ from $w = \beta/\alpha$ to $w = 1$, its value will be determined, for given $t$, by the contribution from the neighbourhood of $w = \beta t/x$. If in that neighbourhood $G(w)$ is changing slowly,
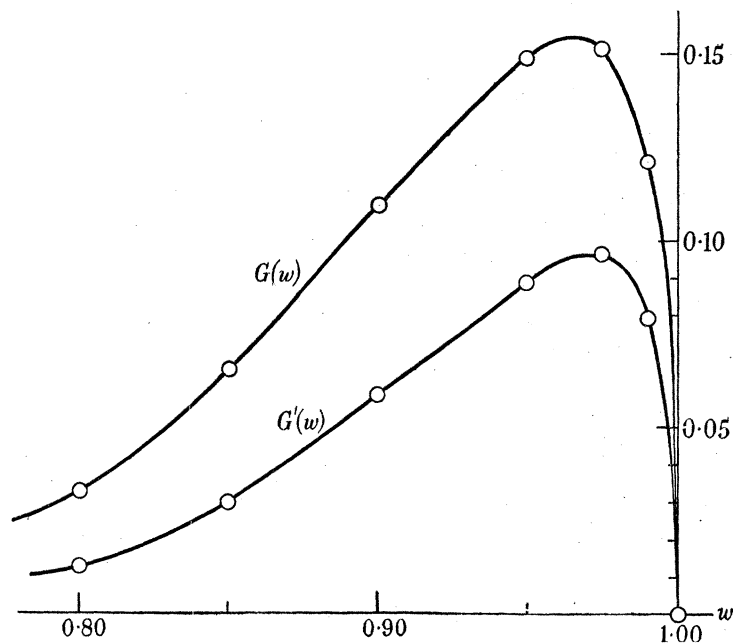


FIGURE 16. $G(w)$ and $G'(w)$.
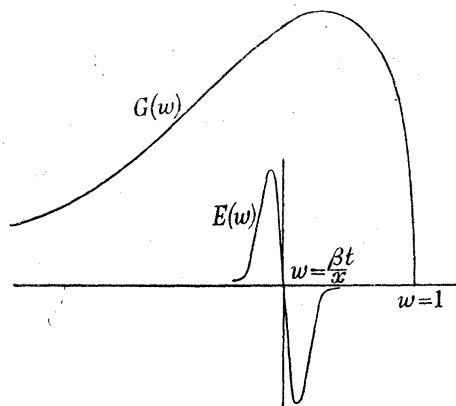


FIGURE 17. $G(w)$ and $E(w)$.
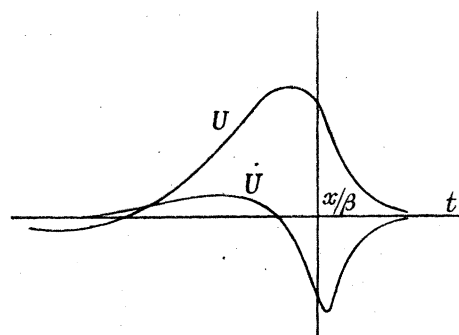


FIGURE 18. $U$ and $\dot{U}$ for $pSp$.

the value of $U$ will be small, but if $G(w)$ is changing fast the value of $U$ may be large. $G(w)$, which is independent of all variables except $w$ and $\beta/\alpha$, is plotted in figure 16 for the Poisson case. From this figure we see immediately that $G(w)$ changes slowly except near $w = 1$, where the change is very rapid. Figure 17 shows $E(w)$ superposed on $G(w)$. The actual position of $E(w)$ depends on the value of $t$; the zero of $E(w)$ moves from $w = \beta/\alpha$ to $w = 1$ as $t$ increases from $x/\alpha$ to $x/\beta$. By imagining the ordinates of the two curves in figure 17 to be multiplied together and the product integrated, we can obtain a qualitative picture of the behaviour of $U$ as $t$ varies. This is sketched in figure 18. In the same figure is graphed the slope of this curve, which gives $\dot{U}$, and can be compared with the result obtained by the previous approximation (figure 14).

The variation in the vertical displacement, $W$, can be discussed in the same way as that of $U$. Approximating on $\Gamma_\beta$ we get

$$\dot{w} \doteq \pm \frac{B\sqrt{\pi}}{\beta_1} i^{-\frac{1}{4}} \omega^{\frac{1}{4}} e^{i\omega\tau \pm p\omega} \quad \text{as} \quad \mathscr{R}(\omega) \lessgtr 0, \tag{14.15}$$

and hence a rough approximation for small $\tau$ and large $x/(z+h)$

$$\dot{W} \doteq -\frac{B}{\beta_1} p^{-\frac{1}{2}} \cos^{\frac{1}{2}} \psi \sin\left(\tfrac{1}{2}\psi - \tfrac{1}{4}\pi\right). \tag{14.16}$$
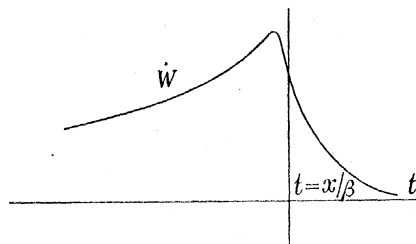
This is plotted in figure 19.



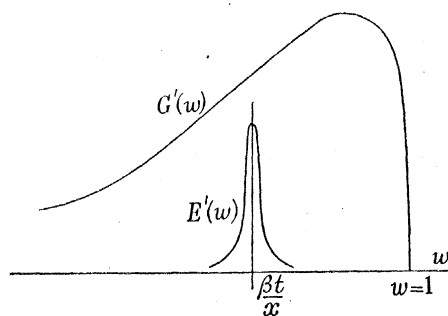FIGURE 19. $\dot{W}$ for $pSp$ from approximation on $\Gamma_\beta$.
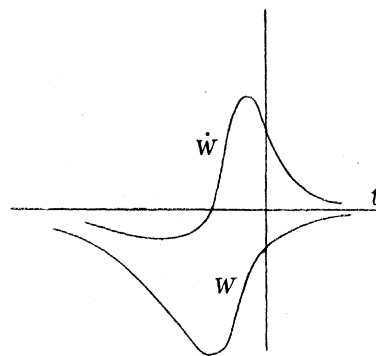


FIGURE 20. $G'(w)$ and $E'(w)$.



FIGURE 21. $W$ and $\dot{W}$ for $pSp$.

When we invert the order of integration, we obtain

$$W = -\frac{16}{\pi} \int_{\beta/\alpha}^{1} G'(w)\, E'(w)\, dw, \tag{14.17}$$

where

$$G'(w) = \frac{w^2 - \beta^2/\alpha^2}{w} G(w), \tag{14.18}$$

and

$$E'(w) = \frac{h+z}{(h+z)^2 (w^2 - \beta^2/\alpha^2) + (\beta t - wx)^2}. \tag{14.19}$$

$E'(w)$ is always positive within the range of integration, with a peak at $w = \beta t/x$ whose sharpness increases as $(h+z)/x$ decreases. $G'(w)$ is plotted in figure 16—its form being similar to that of $G(w)$. Figure 20 shows $E'(w)$ superposed on $G'(w)$, and from this figure we can form a picture of the behaviour of $W$ as $t$ varies, which is sketched, with $W$, in figure 21.

For given $x$, increase of $(h+z)$ lowers and broadens the peak-and-trough of $E(w)$ and the peak of $E'(w)$, and consequently smooths down the irregularity of $U$ and $W$ near $t = x/\beta$. The disturbance is thus confined to the neighbourhood of the surface, though not by an

exponential factor. It cannot, however, travel as a self-sufficient pulse along the surface, preserving its amplitude, since the Rayleigh-pulse alone has this property. Its energy must be continually supplied by the local incident $P$-pulse.

From figures 18 and 21 we see that neither the displacements nor the velocities of the surface $S$-pulse experience a sudden discontinuity; they start from zero and change gradually, unlike those of the surface $P$-pulse $sPs$.

### 15. The secondary $S$- and $P$-pulses

Finally, we have to consider the two very similar expressions $_p\Psi_\beta$ and $_s\Phi_\beta$. We could proceed to find displacements and velocities at a depth $z$, but the expressions for them are very complicated. We therefore simplify the algebra by considering the disturbance associated with $_p\Psi_\beta$ at $z = 0$. Retaining only the first terms

$$\dot{U}_0 \doteqdot 4\sqrt{2}\,\beta^{\frac{3}{2}} x^{-\frac{3}{2}} p^{-\frac{1}{2}} \cos^{\frac{3}{2}}\psi \sin\left(\tfrac{1}{2}\psi + \tfrac{1}{4}\pi\right), \tag{15.1}$$

$$\dot{W}_0 \doteqdot 16\sqrt{2}\,\beta^{\frac{3}{2}}\beta_1^{-1} x^{-\frac{3}{2}} p^{-\frac{1}{2}} \cos^{\frac{5}{2}}\psi \sin\left(\tfrac{1}{2}\psi - \tfrac{1}{4}\pi\right), \tag{15.2}$$

where

$$\tau = t - x/\beta, \quad p = h/\beta_1 \quad \text{and} \quad \psi = \tan^{-1}(\tau/p). \tag{15.3}$$

As with the surface $S$-pulse, (15.1) and (15.2) are valid only in the immediate neighbourhood of $\tau = 0$, and when $x/(h+z)$ is large.

If we now employ the method of the previous section to get a qualitative description of $U_0$ and $W_0$, we obtain, on setting $z = 0$,

$$U_0 = -\frac{8}{\pi\beta}\int_{\beta/\alpha}^1 G_1(w)\,\frac{T}{P^2 + T^2}\,dw, \tag{15.4}$$

$$W_0 = \frac{32}{\pi\beta}\int_{\beta/\alpha}^1 G_1'(w)\,\frac{P}{P^2 + T^2}\,dw, \tag{15.5}$$

where

$$T = t - wx/\beta, \quad P = h\sqrt{(w^2 - \beta^2/\alpha^2)}/\beta,$$

$$\left.\begin{aligned}
G_1(w) &= \frac{w(2w^2 - 1)^3\sqrt{(1 - w^2)}}{(2w^2 - 1)^4 + 16w^4(1 - w^2)(w^2 - \beta^2/\alpha^2)},\\[1em]
G_1'(w) &= \frac{w^4(2w^2 - 1)\sqrt{[(1 - w^2)(w^2 - \beta^2/\alpha^2)]}}{(2w^2 - 1)^4 + 16w^4(1 - w^2)(w^2 - \beta^2/\alpha^2)}.
\end{aligned}\right\} \tag{15.6}$$

and

If diagrams are made from the expressions (15.1) to (15.6) as before, it becomes clear that the disturbance at the surface corresponding to $_p\Psi_\beta$ is of the same type as that given by the surface $S$-pulse.

$_s\Phi_\beta$ is very different. The approximation on $\Gamma_\beta$ is obtained from that for $_p\psi_\beta$ by changing the sign and interchanging $z$ and $h$. If in the resulting expression we put $z = 0$, the exponent becomes

$$i\omega[t - (x + h^2/2x)/\beta], \tag{15.7}$$

and $_s\Phi_\beta$ represents a pulse which arrives at the surface with a sharp jerk in the displacements at time $(x + h^2/2x)/\beta$; it is thus a modification of the direct $S$-pulse. By the usual methods we obtain, when $h/x$ is small,

$$U_0 \doteqdot 4\sqrt{2}\,hx^{-\frac{3}{2}}\beta^{-\frac{1}{2}}\tau^{-\frac{1}{2}} H(\tau), \tag{15.8}$$

$$W_0 \doteqdot -4\sqrt{2}\,hx^{-\frac{3}{2}}\beta_1^{-1}\beta^{\frac{1}{2}}(\tau')^{-\frac{1}{2}} H(\tau'), \tag{15.9}$$

with

$$\tau = t - (x + h^2/2x)/\beta \quad \text{and} \quad \tau' = -\tau. \tag{15.10}$$

The usual shape of the pulse is distorted in $W_0$, as with $SS$.

An interesting check on our methods is obtained by inverting the order of integration in $_s\Phi_\beta$. Retaining $z$, for reasons which become obvious in the course of the algebra, we have, by the usual substitutions,

$$u = -\frac{4}{\pi\beta} \int_{\beta/\alpha}^1 G_2(w)\, dw \int_0^\infty (2A \cos \omega T \sin \omega Q - 2B \cos \omega T \cos \omega Q)\, e^{-\omega P}\, d\omega,$$

where 
$$P = \frac{z}{\beta}\sqrt{(w^2 - \beta^2/\alpha^2)}, \quad Q = \frac{h}{\beta}\sqrt{(1 - w^2)}, \quad T = t - wx/\beta,$$

and 
$$A = (2w^2 - 1)^2, \quad B = 4w^2\sqrt{[(1 - w^2)(w^2 - \beta^2/\alpha^2)]}, \quad G_2 = w^2(2w^2 - 1)/(A^2 + B^2).$$

Splitting up the trigonometric terms we get

$$U = -\frac{4}{\pi\beta} \int_{\beta/\alpha}^1 G_2(w)\, dw \left[ A\left(\frac{T + Q}{P^2 + \overline{T + Q}^2} - \frac{T - Q}{P^2 + \overline{T - Q}^2}\right) - B\left(\frac{P}{P^2 + \overline{T + Q}^2} + \frac{P}{P^2 + \overline{T - Q}^2}\right) \right].$$
(15·11)

Similarly
$$W = -\frac{4}{\pi\beta} \int_{\beta/\alpha}^1 G_2'(w)\, dw \left[ A\left(\frac{P}{P^2 + \overline{T + Q}^2} - \frac{P}{P^2 + \overline{T - Q}^2}\right) - B\left(\frac{T + Q}{P^2 + \overline{T + Q}^2} + \frac{T - Q}{P^2 + \overline{T - Q}^2}\right) \right],$$
(15·12)

where
$$G_2'(w) = \frac{\sqrt{(w^2 - \beta^2/\alpha^2)}}{w}\, G_2(w).$$

If now we put $z = 0$, $P = 0$, and (15·11) and (15·12) reduce to

$$U_0 = \frac{8}{\pi\beta} \int_{\beta/\alpha}^1 G_2(w)\, dw\, \frac{AQ}{T^2 - Q^2},$$
(15·13)

$$W_0 = \frac{8}{\pi\beta} \int_{\beta/\alpha}^1 G_2'(w)\, dw\, \frac{BT}{T^2 - Q^2},$$
(15·14)

the expressions 
$$E_2(w) = \frac{Q}{\beta(T^2 - Q^2)} = \frac{h\sqrt{(1 - w^2)}}{(\beta t - wx)^2 - h^2(1 - w^2)},$$
(15·15)

and 
$$E_2'(w) = \frac{T}{\beta(T^2 - Q^2)} = \frac{\beta t - wx}{(\beta t - wx)^2 - h^2(1 - w^2)}$$
(15·16)

become infinite at the two values of $w$ which make the denominator vanish. These are

$$w = \frac{\beta tx \pm h\sqrt{(h^2 + x^2 - \beta^2 t^2)}}{h^2 + x^2}.$$
(15·17)

In general, when $t$ is given, these two values are distinct, and if $w_1$ is one of them, $E_2$ and $E_2'$ behave like $(w - w_1)^{-1}$ at $w_1$. Hence, unless the other factor in the integrand is changing infinitely fast at $w_1$ the integral remains finite (principal values being taken at each discontinuity). The only place where the other factor changes infinitely fast is $w = 1$, and there it is zero, vanishing like $\sqrt{(1 - w)}$. This makes the integrand become infinite like $(1 - w)^{-\frac{1}{2}}$, and consequently the integral converges there.

But if $t = \sqrt{(h^2 + x^2)}/\beta$, $E_2$ and $E_2'$ behave like $(w - w_1)^{-2}$ at $w_1 = x/\sqrt{(x^2 + h^2)}$, and the integral diverges for this value of $t$. Thus the displacements become infinite at time $\sqrt{(h^2 + x^2)}/\beta$ and for no other time, and consequently $_s\Phi_\beta$ represents, at the surface, a sharp pulse of the same shape as the direct and reflected pulses.

It will be noted that if $z$ is not zero, we must revert to the expressions (15·11) and (15·12), which do not become infinite for any value of $t$. This pulse is sharp only on the surface, and fades out as the depth increases. At the surface it is simply a modification of the disturbance created by the incident $S$-pulse and the reflected pulse $SS$.

## 16. CONCLUSIONS

We now collect the results of the previous sections, in order to envisage the sequence of pulses which arrive at the point $G$, taking $h$ and $z$ to be small compared with $x$. To economize description we refer to a displacement which starts with an infinite discontinuity, and tails off to zero or a finite value, as a 'jerk', whereas a displacement without discontinuities in extent or gradient, but evidencing the passage of a pulse, will be called a 'blunt pulse'.

### I. Initial P-pulse

Let the initial pulse be a cylindrical explosion at $F$. In an infinite solid this would cause an irrotational jerk at $G$, with a residual displacement inversely proportional to $\varpi$ (§4). Then in the semi-infinite solid the following sequence of pulses arrives at $G$:

(a) Direct $P$-pulse $P$ (given by $_p\Phi_0$, arriving at $t = \varpi/\alpha$). This is a jerk whose amplitude at a given time $\tau$ after onset varies at $\varpi^{-\frac{1}{2}}$ (§4).

(b) Reflected $P$-pulse $PP$ ($-_p\Phi_r + _p\Phi_\alpha, t = \varpi'/\alpha$): a jerk of opposite sign from $P$, coming from the image source, and smaller in amplitude by a factor which is $[1 - 8\sqrt{2}\,(h+z)/x]$ (for the Poisson case) when $(h+z)/x$ is small (§11).

(c) Reflected $S$-pulse $PS$ ($_p\Psi_\alpha, t = x/\alpha + z/\beta_1 + \frac{1}{2}h^2/(\alpha x - \beta_1 z)$): a jerk. The ratio of the amplitudes of $_p\Psi_\alpha$ and $_p\Phi_0$ varies as $h/x$, so that $PS$ is small when the focus is shallow. The displacement at $\tau$ is proportional to $x^{-\frac{3}{2}}$ (§11).

(d) Surface $S$-pulse $pSp$ ($_p\Phi_\beta, t = x/\beta$): a blunt pulse, whose displacements and velocities show peaks whose magnitude is inversely proportional to $x(h+z)$. This is a true surface-pulse in that it is confined to the near neighbourhood of $z = 0$, but it is not able to propagate itself, and depends on energy supplied by the incident $P$-pulse. It is insignificant unless both $h$ and $z$ are small (§14).

(e) Secondary $S$-pulse $pS$ ($_p\Psi_\beta, t = \sqrt{(x^2 + z^2)}/\beta$). This is like $pSp$ except that attenuation depends only upon $h$ and not on $z$. It is a minor disturbance due to the propagation through the solid of a distortion set up at the surface near the epicentre (§15).

(f) Rayleigh-pulse $R$ ($_p\Phi_\gamma + _p\Psi_\gamma, t = x/\gamma$): a blunt pulse, attenuated like $[(h+z)/\gamma_\alpha]^{-1}$ (irrotational part) or $[h/\gamma_\alpha + z/\gamma_\beta]^{-1}$ (distortional part). This is a true surface wave, which loses no energy to the interior of the elastic solid, but proceeds with undiminished amplitude in the direction of $x$ (§12).

### II. Initial S-pulse

If the initial pulse is purely distortional, the sequence of pulses at $G$ is:

(a) Reflected $P$-pulse $SP$ ($_s\Phi_\alpha, t = x/\alpha + h/\beta_1 + \frac{1}{2}z^2/(\alpha x - \beta_1 h)$): a jerk, from reflexion near the epicentre. Since $_s\Phi_\alpha/_s\Psi_0 \propto z/x$, it is small when $z$ is small (§11).

(b) Surface $P$-pulse $sPs$ ($_s\Psi_\alpha, t = x/\alpha + (h+z)/\beta_1$). This is not a true surface wave, but is more like a body wave reflected twice at the surface. The path is a minimum-time path, travelled with velocity $\beta$ to and from the surface, but with velocity $\alpha$ along the surface. The

displacement of $G$ is continuous, but there is a jerk in velocity. Thus the displacement has a definite instant of beginning. The amplitude at time $\tau$ varies like $x^{-\frac{3}{2}}$ approximately (§ 13).

($c$)  Direct $S$-pulse $S$ ($_s\Psi_0$, $t = \varpi/\beta$): a jerk, amplitude at time $\tau$ after onset varying as $\varpi^{-\frac{1}{2}}$ (§§ 4 and 11).

($d$)  Secondary $P$-pulse $sP$ ($_s\Phi_\beta$, $t = \surd(x^2+h^2)/\beta$) is a blunt pulse except when $G$ is at the surface. Then it becomes part of the complicated disturbance at the arrival of the $S$-pulse (§ 15).

($e$)  Reflected $S$-pulse $SS$ ($_s\Psi_\beta - {_s\Psi_r}$, $t = \varpi'/\beta$): this is remarkable in that the jerk given by $_s\Psi_\beta$ is turned approximately back-to-front—a consequence of the change of phase of each element of its spectrum on reflexion at the surface. The total displacement is given by the addition of this to $- {_s\Psi_r}$, which is a pulse opposite in sign to the initial pulse and proceeding from the image point. Since the ratio of the displacements is proportional to $(h+z)/x$ the modification of $- {_s\Psi_r}$ is small at large distances (§ 11).
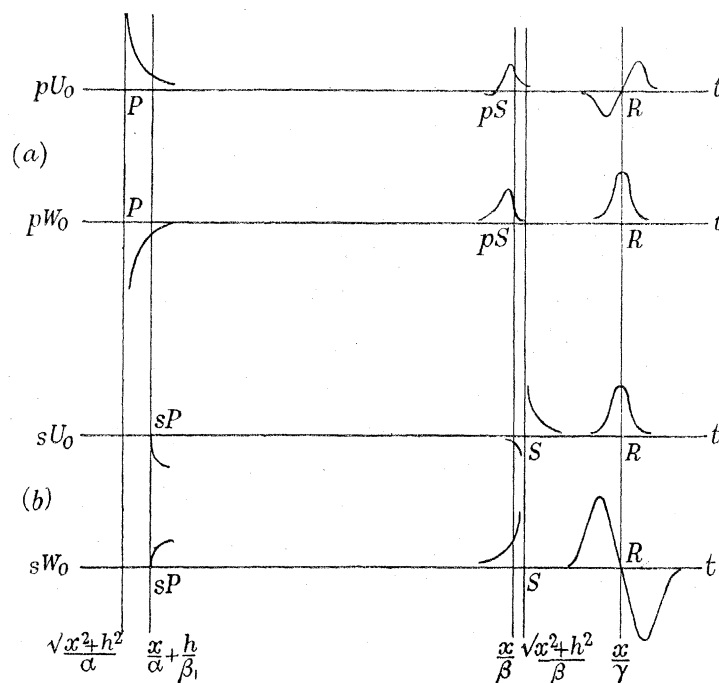


FIGURE 22.  Horizontal ($U_0$) and (downward) vertical ($W_0$) displacements due to
($a$) initial $P$-pulse and ($b$) initial $S$-pulse.

($f$)  Rayleigh-pulse $R$ ($_s\Phi_\gamma + {_s\Psi_\gamma}$, $t = x/\gamma$): a blunt pulse, attenuated like $[h/\gamma_\beta + z/\gamma_\alpha]^{-1}$ (irrotational part) and $[(h+z)/\gamma_\beta]^{-1}$ (distortional part) (§ 12).

Of the above effects, I ($a$), ($b$), ($c$) and II ($a$), ($c$), ($e$) are the same as those which would arise from an incident plane wave, whereas I ($d$), ($e$), ($f$) and II ($b$), ($d$), ($f$) are diffraction phenomena, due to the curvature of the wave-fronts. Of these the Rayleigh-pulse is clearly the most important.

We are interested especially in the surface disturbances, derived by putting $z = 0$ in the above work. Then for an initial $P$-pulse, $P$, $PP$ and $PS$ combine, and $pS$, $pSp$ combine. For an initial $S$-pulse $sPs$ combines with $SP$, and $S$, $SS$ and $sP$ combine. The approximations for $U$ and $W$ at $z = 0$ on arrival of the various pulses are shown in tables 1 and 2 in order

of occurrence. Figure 22 (*a*) and (*b*) correspond to these tables, indicating the time of arrival and the approximate form near that time for each pulse.

Figure 22 cannot give more than a rough sketch of the main features of the disturbance at $G$, on account of the approximations of this work, but several points of interest emerge.

### TABLE 1. INITIAL $P$-PULSE

| pulse | | time of arrival | approximations valid when $\frac{\alpha\tau}{x}$ and $\frac{h+z}{x}$ are small | |
|---|---|---|---|---|
| | | | $U_0$ | $W_0$ |
| $_p\Phi_0$ | $P$ | | $\sqrt{\left(\frac{2}{x\alpha\tau}\right)}H(\tau)$ | $-\frac{h}{x}\sqrt{\left(\frac{2}{x\alpha\tau}\right)}H(\tau)$ |
| $-_p\Phi_r$ | $PP$ | $\frac{\sqrt{(x^2+h^2)}}{\alpha}$ | $-\sqrt{\left(\frac{2}{x\alpha\tau}\right)}H(\tau)$ | $-\frac{h}{x}\sqrt{\left(\frac{2}{x\alpha\tau}\right)}H(\tau)$ |
| $_p\Phi_\alpha$ | $PP$ | | $16\frac{h}{x}\sqrt{\left(\frac{2}{x\alpha\tau}\right)}H(\tau)$ | $16\frac{h^2}{x^2}\sqrt{\left(\frac{2}{x\alpha\tau}\right)}H(\tau)$ |
| $_p\Psi_\alpha$ | $PS$ | | $4\frac{\alpha}{\beta_1}\frac{h}{x}\sqrt{\left(\frac{2}{x\alpha\tau}\right)}H(\tau)$ | $-4\frac{h}{x}\sqrt{\left(\frac{2}{x\alpha\tau}\right)}H(\tau)$ |
| $_p\Phi_\beta$ $_p\Psi_\beta$ | $pSp$ $pS$ | $\frac{x}{\beta}$ | $\frac{8}{\pi}\int_{\beta/\alpha}^1 G_3(w)\,E_3(w)\,dw$ | $\frac{16}{\pi}\int_{\beta/\alpha}^1 G_3'(w)\,E_3'(w)\,dw$ |

where $\quad G_3(w)=\dfrac{w(2w^2-1)^2\sqrt{(1-w^2)}}{(2w^2-1)^4+16w^4(1-w^2)\,(w^2-\beta^2/\alpha^2)^2}, \quad E_3(w)=\dfrac{1}{\beta}\dfrac{T}{P^2+T^2}$

$\qquad G_3'(w)=\dfrac{w^2(2w^2-1)\,\sqrt{[(1-w^2)\,(w^2-\beta^2/\alpha^2)]}}{(2w^2-1)^4+16w^4(1-w^2)\,(w^2-\beta^2/\alpha^2)^2}, \quad E_3'(w)=\dfrac{1}{\beta}\dfrac{P}{P^2+T^2}$

$\qquad T=t-wx/\beta, \quad P=h\sqrt{(w^2-\beta^2/\alpha^2)}/\beta$

| $_p\Phi_\gamma$ $_p\Psi_\gamma$ | $R$ $R$ | $\frac{x}{\gamma}$ | $\frac{1}{\pi}\left(\frac{A_r}{\gamma}-\frac{A_r'}{\gamma_\beta}\right)\frac{\tau}{p^2+\tau^2}$ | $\frac{1}{\pi}\left(\frac{A_r'}{\gamma}-\frac{A_r}{\gamma_\alpha}\right)\frac{p}{p^2+\tau^2}$ |

where $\quad \tau=t-x/\gamma, \quad p=h/\gamma_\alpha$

### TABLE 2. INITIAL $S$-PULSE

| pulse | | time of arrival | approximations valid when $\frac{\alpha\tau}{x}$ and $\frac{h+z}{x}$ are small | |
|---|---|---|---|---|
| | | | $U_0$ | $W_0$ |
| $_s\Phi_\alpha$ $_s\Psi_\alpha$ | $SP$ $sPs$ | $\frac{x}{\alpha}+\frac{h}{\beta_1}$ | $-16\frac{\beta_2^6}{\alpha^3\beta^2\beta_1}\sqrt{\left(\frac{2\alpha\tau}{x^3}\right)}H(\tau)$ | $8\frac{\beta_2^4}{\alpha^2\beta^2}\sqrt{\left(\frac{2\alpha\tau}{x^3}\right)}H(\tau)$ |
| $_s\Psi_0$ | $S$ | | $-\frac{h}{x}\sqrt{\left(\frac{2}{x\beta\tau}\right)}H(\tau)$ | $-\sqrt{\left(\frac{2}{x\beta\tau}\right)}H(\tau)$ |
| $-_s\Psi_r$ | $SS$ | $\frac{\sqrt{(x^2+h^2)}}{\beta}$ | $-\frac{h}{x}\sqrt{\left(\frac{2}{x\beta\tau}\right)}H(\tau)$ | $\sqrt{\left(\frac{2}{x\beta\tau}\right)}H(\tau)$ |
| $_s\Phi_\beta$ | $sP$ | | $4\frac{h}{x}\sqrt{\left(\frac{2}{x\beta\tau}\right)}H(\tau)$ | $-4\frac{\beta}{\beta_1}\frac{h}{x}\sqrt{\left(\frac{2}{x\beta\tau'}\right)}H(\tau')$ |
| $_s\Psi_\beta$ | $SS$ | | $-8\frac{\beta}{\beta_1}\frac{h^2}{x^2}\sqrt{\left(\frac{2}{x\beta\tau'}\right)}H(\tau')$ | $8\frac{\beta}{\beta_1}\frac{h}{x}\sqrt{\left(\frac{2}{x\beta\tau'}\right)}H(\tau')$ |

$\tau'=-\tau$

| $_s\Phi_\gamma$ $_s\Psi_\gamma$ | $R$ $R$ | $\frac{x}{\gamma}$ | $\frac{1}{\pi}\left(\frac{A_r'}{\gamma}-\frac{A_r}{\gamma_\alpha}\right)\frac{q}{q^2+\tau^2}$ | $-\frac{1}{\pi}\left(\frac{A_r\gamma_\beta}{\gamma\gamma_\alpha}-\frac{A_r'}{\gamma_\alpha}\right)\frac{\tau}{q^2+\tau^2}$ |

where $\quad \tau=t-x/\gamma, \quad q=h/\gamma_\beta$

These tables are illustrated in figure 22, which shows the time of arrival and the approximate form near that time for each pulse.

The arrival of $P$ and the surface $P$-pulse occurs in each case at a definite instant; the surface $S$-pulse and $S$, on the other hand, show no definite beginning, growing slowly out of the previous disturbance. $S$, however, is a modified jerk, while $pS$ is a blunt pulse.

The general reciprocity between the consequences of initial $P$- and initial $S$-pulse is most clearly shown in the Rayleigh-pulse—the coefficient in $_pW_0$ is equal to that in $_sU_0$ while the ratio of the coefficients in $_pU_0$ and $_pW_0$ is equal to the corresponding ratio in $_sU_0$ and $_sW_0$. This can be proved by inserting the values of $A$ and $A'$ and using the equation which gives the velocity of the Rayleigh-wave.

The reality of the two surface-pulses first suggested by Nakano seems to be proved by this investigation, and their difference brought out more clearly. The surface $P$-pulse is like a doubly reflected pulse, shows a definite beginning, and is not sensitive to depth of focus. The surface $S$-pulse, on the other hand, has no definite beginning, resembles the Rayleigh-pulse except in its failure to persist in its own right, and is very sensitive to depth of focus. Nakano's failure to find this pulse by his second method (stationary phase) seems to have been due to his overlooking a loop on the Riemann surface.

The diffraction effects examined in this paper can be described as pulses only when $h/x$ is small, and our description of the disturbance is only valid in the neighbourhood of the critical instants when the pulses arrive. If $h/x$ is not small, the diffraction pattern is very complicated and smudged; pulses will not be discernible. Earthquake shocks, however, are nearly always observed at distances such that $h/x$ is small, so that this case is the one that concerns us.

Although our results have been obtained on a very restricted hypothesis, there is reason to believe that they may apply in some degree to the phenomena of near earthquakes. For such the neglect of the curvature of the earth introduces a small error only. Our hypothesis of a homogeneous semi-infinite solid means that our work cannot account for phenomena which are due to stratification (such as Love waves) or variation of velocity with depth, but those pulses which it does predict should also appear in the more complicated cases. The specialized form which we have taken for the initial pulse has been shown by Jeffreys (1931) to be a fair representation of the shock for a wide class of earthquakes.

The treatment of the two-dimensional problem in place of the true three-dimensional one means that we deal with cylindrical wavefronts instead of the true spherical ones. Lamb showed, however, in a similar problem (1904) that the general form of resultant disturbance at a point of the surface is the same in the two cases, the main differences lying in the different law of decrease of amplitude with distance, and in the cutting off of the infinite tails which appear in the two-dimensional case. The essential features of our solution may consequently be expected to appear in the three-dimensional problem.

Explanations may therefore be suggested for two apparent anomalies in earthquake records: (a) seismograms of near earthquakes sometimes show $Sg$ as having arrived 1 to 2 sec. before the time at which it would be expected after $Pg$ (Jeffreys 1929, p. 98), and also (b) 'up to about 20°, the $S$ residuals are spread over about 20 sec. without any convincing concentration of frequency' (Jeffreys 1946, p. 61). Here $Sg$, $Pg$ and $S$ have their usual meanings in seismology. In view of these facts it is worth while to examine in further detail the form of our $S$ and $pS$, in order to find out how long before the instant $t = \sqrt{(x^2+h^2)}/\beta$ the disturbance might become perceptible.

The question cannot be answered directly from our previous discussion, since our simplifying assumption of an instantaneous shock at the focus leads to an infinite displacement at the time of arrival of a jerk at $G$. Let us therefore modify our assumption of time variation as $H(t)$ to time variation as

$$\tan^{-1}\frac{t}{s} = \int_0^\infty e^{-s\omega}\sin\omega t\,\frac{d\omega}{\omega}. \tag{16.1}$$

(16.1) has the limit $\frac{1}{2}\pi\,\mathrm{sgn}\,t$ as $s\to 0$. About 70 % of the total change in $\tan^{-1}t/s$ takes place between the values $\pm 2s$ of $t$. This change in our assumption will mean that certain terms previously neglected must now be taken into account, but the work follows exactly the methods used in §§ 11 and 14. Collecting all the terms which contribute to the disturbance near $t = x/\beta$ we obtain for the rates of displacement at the surface, by the approximation for large $x/h$ and small $\tau$:

$$\dot{U}_0 \doteq \frac{\sqrt{(2\beta)}\,\pi}{x^{\frac{3}{2}}}\left\{\frac{8\beta}{\beta_1}\frac{\sin\left(\frac{1}{2}\psi-\frac{1}{4}\pi\right)}{(s^2+\tau^2)^{\frac{1}{4}}} - \frac{h}{\beta}\frac{\sin\left(\frac{3}{2}\psi-\frac{1}{4}\pi\right)}{(s^2+\tau^2)^{\frac{3}{4}}} - \frac{4}{\beta_1}\frac{h^2}{x}\frac{\sin\left(\frac{3}{2}\psi+\frac{1}{4}\pi\right)}{(s^2+\tau^2)^{\frac{3}{4}}} - 4\frac{\sin\left(\frac{1}{2}\psi'+\frac{1}{4}\pi\right)}{[(s+p)^2+\tau'^2]^{\frac{1}{4}}}\right\}, \tag{16.2}$$

$$\dot{W}_0 \doteq \frac{2\sqrt{(2\beta)}\,\pi\beta}{x^{\frac{3}{2}}\beta_1}\left\{\frac{8\beta}{\beta_1}\frac{\sin\left(\frac{1}{2}\psi+\frac{1}{4}\pi\right)}{(s^2+\tau^2)^{\frac{1}{4}}} - \frac{h}{\beta}\frac{\sin\left(\frac{3}{2}\psi+\frac{1}{4}\pi\right)}{(s^2+\tau^2)^{\frac{3}{4}}} + \frac{4}{\beta_1}\frac{h^2}{x}\frac{\sin\left(\frac{3}{2}\psi-\frac{1}{4}\pi\right)}{(s^2+\tau^2)^{\frac{3}{4}}} + 4\frac{\sin\left(\frac{1}{2}\psi'-\frac{1}{4}\pi\right)}{[(s+p)^2+\tau'^2]^{\frac{1}{4}}}\right\}, \tag{16.3}$$

where

$$\tau = t - \frac{1}{\beta}\left(x+\frac{h^2}{2x}\right), \quad \psi = \tan^{-1}\frac{\tau}{s}, \tag{16.4}$$

$$\tau' = t - \frac{x}{\beta}, \quad p = \frac{h}{\beta_1} \quad \text{and} \quad \psi' = \tan^{-1}\frac{\tau'}{s+p}. \tag{16.5}$$

(We deal in each case with a rate of displacement because it is a change in this quantity rather than in the displacement which indicates to an observer the arrival of a pulse.)

In each of (16.2) and (16.3) the first three terms describe the arrival of $S$, and the last the arrival of $pS$. The times of arrival, given in (16.4) and (16.5), are not identical, but for practical purposes their difference may be neglected. In each equation the second and third terms give a significant contribution only in the immediate neighbourhood of $\tau = 0$, but the first and fourth have a much wider spread. $-\sin\left(\frac{1}{2}\psi+\frac{1}{4}\pi\right)/(s^2+\tau^2)^{\frac{1}{4}}$ has the shape shown in figure 14: on the steep side of the trough the ordinate falls to 20 % of its largest numerical value within $\tau/s = -2$, whereas on the gentler slope the same value of the ordinate occurs at $\tau/s = 38$. The first term of $\dot{U}_0$ and the fourth of $\dot{W}_0$ are like the reflexion of this in the line $t = 0$, and so they rise to 20 % of their numerical maximum when $\tau/s = -38$. The first and last terms will dominate the middle terms when $h$ is very small and $s$ is not too small. $s$ is the parameter which determines the sharpness of the shock at the focus. If we suppose that shock to have had a duration of the order of 1 sec., we may take $s = \frac{1}{4}$, and then if $h\beta_1/8\beta^2 s$ is of the order of unity, or smaller, the rate of displacement will attain 20 % of its maximum at times of the order of 10 sec. before and after $x/\beta$. As $h$ increases or $s$ decreases this spread of the pulse contracts.

The above argument holds only for large values of $x/(h+z)$. As a check on it we may carry through the discussion of $\dot{U}_0$ and $\dot{W}_0$ by our second method.

To simplify the analysis, we work for the case when $h$ is negligible and obtain

$$\dot{U}_0 = \int_{\beta/\alpha}^{1} \frac{dw}{\beta} \left[ -M_2 \frac{2sT}{(s^2+T^2)^2} + M_1 \frac{s^2-T^2}{(s^2+T^2)^2} \right], \tag{16.6}$$

$$\dot{W}_0 = \int_{\beta/\alpha}^{1} \frac{dw}{\beta} \left[ -M_3 \frac{s^2-T^2}{(s^2+T^2)^2} - M_2 \frac{2sT}{(s^2+T^2)^2} \right], \tag{16.7}$$

where
$$T = t - \frac{wx}{\beta},$$

$$M_1 = (2w^2-1)^2 N, \tag{16.8}$$

$$M_2 = 2w(2w^2-1)\sqrt{(w^2-\beta^2/\alpha^2)} N, \tag{16.9}$$

$$M_3 = 4w^2(w^2-\beta^2/\alpha^2) N, \tag{16.10}$$

with
$$N = \frac{8w\sqrt{(1-w^2)}}{(2w^2-1)^4 + 16w^4(w^2-\beta^2/\alpha^2)(1-w^2)}.$$

By a discussion like that of §14 it can be shown that while the integrals containing $M_1$ and $M_3$ are small until $t$ is very near $x/\beta$, those containing $M_2$ attain just under 20% of their value at $t = x/\beta$ when $t = 0.97x/\beta$. Thus the disturbance may become perceptible at a time of the order of $0.03x/\beta$ sec. in advance of the time $x/\beta$. This amounts to about 1.8 sec. at 200 km. and 9 sec. at 1000 km. These figures can only be regarded as giving an order of magnitude, but they are of the same order as the observed scatter in the readings of $S_g$ and $S$. Instances of early arrival of $S_g$ might therefore be explained directly by the existence of $pS$ and the form of our $S$-pulse. The scatter of the $S$-pulse of seismology, which has a more complex history than any considered here, may be due to similar reasons.

## REFERENCES

Bromwich, T. J. I'A. 1898  *Proc. Lond. Math. Soc.* **30**, 98–120.

Byerly, P. 1940  *Trans. Amer. Geoph. Un.* **4**, 1117.

Copson, E. T. 1935  *Functions of a complex variable.* Oxford: Clarendon Press.

Fu, C. Y. 1947  *Geophysics,* **12**, 57–71.

Jahnke, E. & Emde, F. 1945  *Tables of functions,* 4th ed.  New York: Steckert.

Jeffreys, H. 1926*a*  *Proc. Camb. Phil. Soc.* **23**, 472–481.

Jeffreys, H. 1926*b*  *Mon. Not. R. Astr. Soc. Geophys. Suppl.* **1**, 321–334.

Jeffreys, H. 1929  *The Earth,* 2nd ed.  Cambridge Univ. Press.

Jeffreys, H. 1931  *Beitr. Geophys.* **30**, 336–350.

Jeffreys, H. 1946  *Rep. Progr. Phys.* **10**, 52–82.

Jeffreys, H. & B. S. 1946  *Methods of mathematical physics.*  Cambridge Univ. Press.

Lamb, H. 1904  *Phil. Trans.* A, **203**, 1–42.

Lamb, H. 1932  *Hydrodynamics,* 6th ed.  Cambridge Univ. Press.

Love, H. 1906  *Mathematical theory of elasticity,* 2nd. ed.  Cambridge Univ. Press.

Muskat, M. 1933  *Physics,* **4**, 14–28.

Nakano, H. 1925  *Jap. J. Astr. Geophys.* **2**, 233–326.

Sommerfeld, A. 1909  *Ann. Phys., Lpz.,* **28**, 665–736.

Stewart, C. A. 1940  *Advanced calculus.*  London: Methuen.